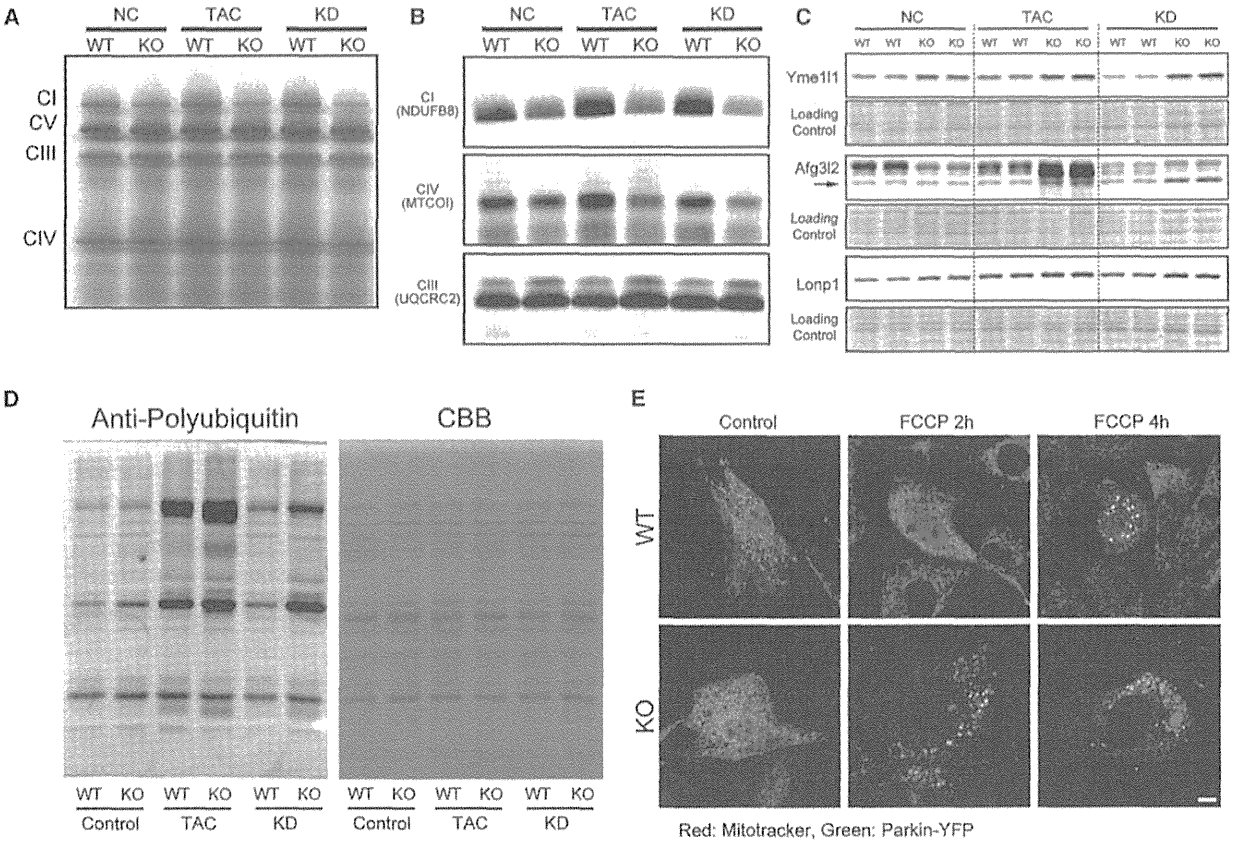

(legend on next page)

results demonstrate that stress-induced mitochondrial remodeling impaired mitochondrial protein synthesis and accelerated the decomposition of respiratory complexes, which triggered the mtUPR and mitophagy in KO mice. Thus, the accumulation of compromised mitochondria ultimately contributes to the development of myopathy and cardiac dysfunction.

Association of ms^2 Modification with Mitochondrial Disease

Because the pathological phenotypes of KO mice resembled those of mitochondrial disease, we speculated that ms^2 modification might be involved in mitochondrial disease. We investigated the ms^2 modification level in peripheral blood cells collected from MELAS patients who carry the A3243G mutation (Figure S7A). Because of the limited number of clinical RNA samples, we adapted the quantitative PCR-based method (Xie et al., 2013), which was originally developed to examine the ms^2 level of ms^2t^6A in cytosolic $tRNA^{Lys(UUU)}$, to sensitively examine the ms^2 modification level ms^2i^6A in mt-tRNAs (Figures S7B–S7E). Strikingly, the heteroplasmy level of mutant mt-DNA was significantly correlated with the ms^2 modification levels of four mt-tRNAs, but not with the cytosolic tRNALys(UUU) (Figures 7A–7D and S7F). Interestingly, the mutant mtDNA level was not correlated with the expression level of *CDK5RAP1*, suggesting that the decrease in ms^2 modifications was not due to a deficiency in Cdk5rap1 (Figures S5D–S5G). Because the A3243G mutation is located in the mtDNA region corresponding to $mt\text{-}tRNA^{Leu(UUR)}$, the decrease in the ms^2 levels of $tRNA^{Trp}$, $tRNA^{Phe}$, $tRNA^{Tyr}$, and $tRNA^{Ser(UCN)}$ was likely not caused by the A3243G mutation but, rather, was due to secondary effects. Cells bearing A3243G mutations in mtDNA exhibit a marked reduction of mitochondrial protein synthesis and an increase in the oxidative stress level (Crimi et al., 2005; Ishikawa et al., 2005). Because Cdk5rap1 contains highly oxidation-sensitive [4Fe-4S] clusters (Arragain et al., 2010), we speculated that the excess oxidative stress originated from mutant mitochondria might result in a collateral inhibition of Cdk5rap1 activity. Indeed, cells treated with sublethal doses of H_2O_2 showed a rapid decrease in ms^2 modification, which was completely reversed by adding 10 mM pyruvate, which serves as an antioxidant (Figures 7E–7G). In addition, treatment of cells with an NO donor such as SNAP and NOC18 significantly reduced the ms^2 modification level, which was reversed by the addition of the NO scavenger PTIO (Figure 7H). Taken together, these results suggest that oxidative stress-induced decreases in ms^2 modifications might compromise the quality of the mitochondria and contribute to the progression of mitochondrial disease.

DISCUSSION

Regulation of Mitochondrial Protein Synthesis by Cdk5rap1-Mediated ms^2 Modification

In the present study, we revealed the important physiological functions of ancient mitochondrial ms^2 modifications in mice and human. Using Cdk5rap1 KO mice, we provide direct evidence that Cdk5rap1 catalyzes the ms^2 modifications of $mt\text{-}tRNA^{Phe}$, $mt\text{-}tRNA^{Trp}$, $mt\text{-}tRNA^{Tyr}$, and $mt\text{-}tRNA^{Ser(UCN)}$ in mammalian cells. The ms^2 group at the A37 of tRNA can directly participate in crossstrand stacking with the first nucleotide of the codon of the mRNA to maintain the reading frame (Jenner et al., 2010). Indeed, a deficiency in the ms^2 modification of ms^2i^6A impaired reading frame maintenance in bacteria and caused defective mitochondrial protein synthesis in Cdk5rap1 KO mice. Interestingly, nuclear-encoded mitochondrial protein, such as NDUFB8 in complex I, was also decreased in KO mice. The indirect decrease of NDUFB8 is most likely due to the poorly assembled respiratory complexes in KO mice. A previous study has shown that a deficiency in a single subunit in complex I could compromise complex formation and cause the proteolysis of other subunits (Karamanlidis et al., 2013). Our results thus demonstrate that the ms^2 modification of mt-tRNAs is indispensable for mitochondrial protein synthesis and the proper assembly of respiratory complexes.

Whereas only one transcript of *Cdk5rap1* has been found in mice, multiple splicing variants of human *CDK5RAP1* are listed in the database (Figure S1A). One transcript of human *CDK5RAP1* encodes a short form of CDK5RAP1 without a mitochondrial localization signal (Q95SZ6-2 in Figure S1A), which raises the possibility that CDK5RAP1 might regulate cellular function by modifying cytosol RNAs (Reiter et al., 2012). However, there was no detectable ms^2i^6A in total RNA isolated from KO MEF cells expressing the cytosolic form of Cdk5rap1 with the enzyme activity preserved. These results clearly suggest that Cdk5rap1 does not modify nuclear DNA-derived RNAs in murine cells. Furthermore, the defective mitochondrial protein synthesis observed in Cdk5rap1 KO mice may be directly caused by the loss of ms^2 modifications in mt-tRNAs.

Deficiency of ms^2 Modification and Its Physiological Outcome

This study revealed unique phenotypic outcomes of Cdk5rap1 KO mice in response to distinct environmental conditions. Under sedentary conditions, the skeletal and cardiac functions of the

Figure 6. The Deficiency in ms^2 Modification Compromises Mitochondrial Protein Quality under Stressed Conditions

(A) Steady-state levels of CI, CIII, CIV, and CV in heart tissue in WT and KO mice treated with NC, KD, and TAC surgery were examined by BN-PAGE.

(B) The steady-state levels of CI protein NDUFB8, CIV protein MTCOI, and CIII protein UQCRC2 in heart tissue in WT and KO mice treated with NC, KD, and TAC surgery were examined by BN-PAGE followed by western blotting. UQCRC2 was used as a loading control.

(C) The protein levels of Yme1l1, Afg 3l2, and Lonp1 were examined in heart tissues from WT and KO mice treated with NC, KD, and TAC surgery. Membranes stained with CBB were used as a loading control.

(D) Enhanced polyubiquitination was observed in the mitochondria in the hearts of KO mice under each stress.

(E) WT and KO cells transfected with Parkin-YFP were treated with 10 μM FCCP for 2 and 4 hr; bar, 10 μm.

(F) WT and KO cells were treated with 10 μM FCCP for 2 and 4 hr. The cells were then stained with an anti-LC3 antibody and Mitotracker. The inserted box shows mitochondria surrounded by the LC3 protein and is magnified in the bottom panels; bar, 10 μm.

(G) Electron microscopy of mitochondria in heart tissue from WT and KO mice treated with KD or TAC surgery. Arrows indicate the autophagic vacuoles; bar, 10 μm.

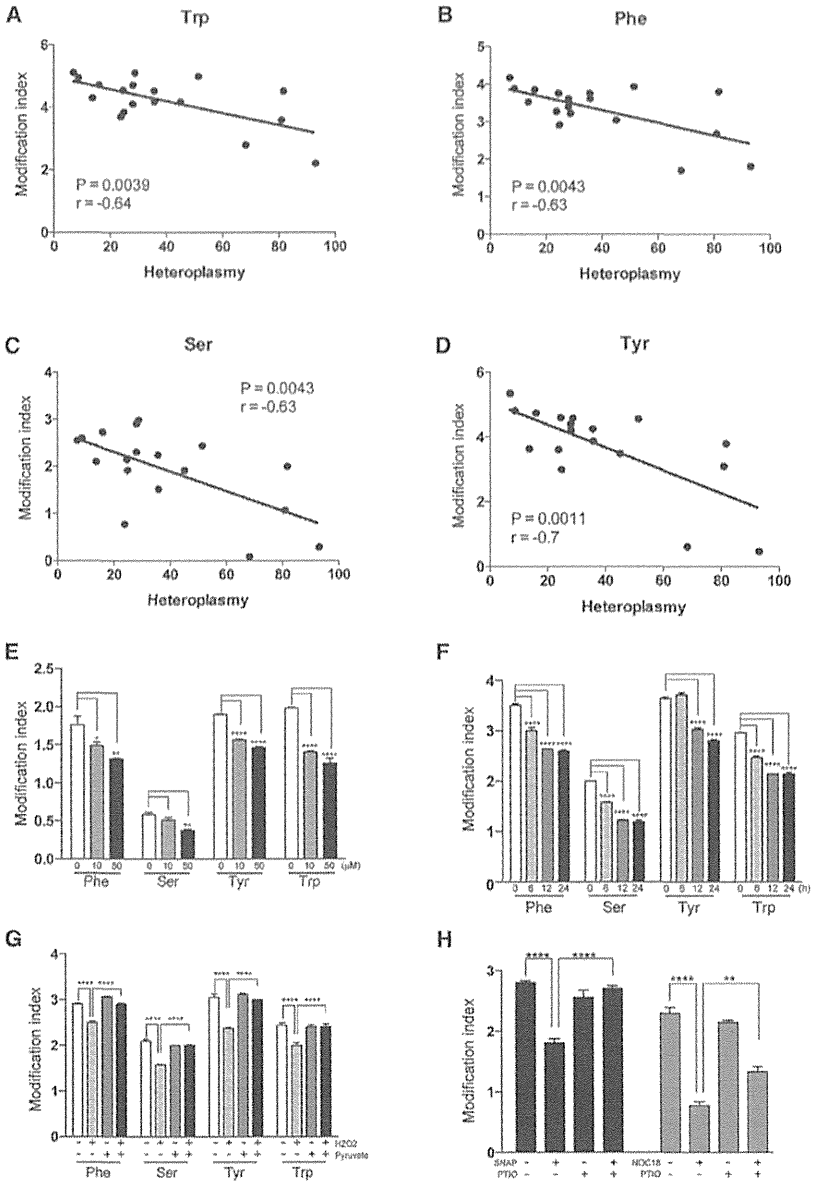

Figure 7. Association of ms^2 Modifications with MELAS

(A–D) Negative correlation of the ms^2 modification level of mt-tRNA^{Trp} (A), mt-tRNA^{Phe} (B), mt-tRNA$^{Ser(UCN)}$ (C), or mt-tRNA^{Tyr} (D) with the heteroplasmy level in MELAS patients; n = 18 each.

(E) Treatment with H_2O_2 reduced the level of ms^2 modification of mt-tRNAs in HeLa cells. Cells were treated with 10 μM or 50 μM H_2O_2 for 24 hr, and the ms^2 modification levels were examined by qPCR; n = 4 each.

(F) Time-dependent decreases in ms^2 modification after H_2O_2 treatment in HeLa cells. Cells were treated with 50 μM H_2O_2 for 6, 12, and 24 hr; n = 4 each.

(G) HeLa cells were treated with 50 μM H_2O_2 for 24 hr in the presence or absence of 10 mM pyruvate. The decrease in the ms^2 modification level was prevented by pyruvate; n = 4 each.

(H) HeLa cells were treated with NO donors, 100 μM SNAP or 100 μM NOC18 for 24 hr in the presence or absence of PTIO. The ms^2 modification level of mt-tRNA^{Trp} was examined by qPCR; n = 4 each. Data are the mean ± SEM. *p < 0.05. **p < 0.01, ****p < 0.0001.

Cdk5rap1 KO mice were compatible with those of the WT mice, despite the marked decrease in respiratory activities and regardless of the increase of oxidative stress. The mitochondrial dysfunction in KO mice might be compensated by the remodeling of mitonuclear protein balance, which serves as a protective mechanism by inducing mtUPR (Houtkooper et al., 2013). Indeed, in contrast to the decrease of mitochondrial protein synthesis, several cytosolic proteins appear to be upregulated in KO cells (right panels in Figure 2A). This mitonuclear protein imbalance might contribute to the upregulation of basal mtUPR in muscle and heart tissues of KO mice (Figure 6C). Furthermore, a collective increase of ROS metabolism genes, including ROS scavenger genes such as *ApoE*, *DHCR24*, and *SRXN1*, might ameliorate oxidative stress and protect the muscular and cardiac functions in KO mice. Similar to our results, previous studies have found no adverse phenotypes under basal conditions in transgenic mice with respiratory defects (Karamanlidis et al., 2013; Wenz et al., 2009). Our results thus support the current perspective that mitochondrial dysfunction, depending on its degree, may not immediately produce a pathological phenotype under sedentary conditions.

In contrast, under stressed conditions, Cdkrap1 KO mice exhibited apparent skeletal muscle and heart dysfunctions. The defective mitochondrial protein synthesis caused a marked decrease in protein levels and activities of complexes I and IV in KO mice under stressed conditions. The progressive disruption of respiratory complexes, which exaggerates mtUPR and mitophagy, thus largely compromised mitochondria quality and led to myopathy in KO mice. Recent studies have shown that Parkin-mediated mitophagy is critical for the removal of damaged mitochondria and thus protects cardiac function under stressed conditions (Hoshino et al., 2013; Chen and Dorn, 2013). However, given the observation of a number of degenerated mitochondria in KO mice (Figures 4D and 5G), the extent of mitochondria damage in KO mice was likely beyond the maintenance capacity of mitophagy, which ultimately led to catastrophic mitochondrial dysfunction and myopathy. In addition, the acceleration of complex I defect was associated with a modest increase of oxidative stress, which could trigger mtUPR and cause cytotoxicity in stressed KO mice (Runkel et al., 2013). However, compared with the progressive impairment of mitochondria quality, the degree of increase of ROS after mitochondrial stress was rather small in

stressed KO mice. Our results thus suggest that ROS might also contribute to the pathogenesis, but to a limited extent. The accumulation of malfunctioning mitochondria is likely the primary cause of the progression of myopathy in KO mice.

Regulation of ms^2 Modification by Oxidative Stress and Its Association with Human Disease

An important finding of this study is that the ms^2 modification levels were reduced in MELAS patients carrying the A3243G mutation in mt-$tRNA^{Leu}$. This result is surprising because mt-$tRNA^{Leu}$ does not contain an ms^2 modification. Previous studies have shown that the deficiency of taurine modification in mt-$tRNA^{Leu}$ carrying the A3243G mutation is the primary cause of MELAS (Kirino et al., 2005; Yasukawa et al., 2001). Given the significant association of the heteroplasmy level with the ms^2 modification level in MEALS patients, our results suggest that the myopathy in MELAS is caused not only by a decoding error at the Leu codon but also by decoding errors occurring at multiple codons, including Leu, Phe, Tyr, Trp, and Ser codons.

The reason A3243G in mt-$tRNA^{Leu}$ is associated with decreased modifications in other mt-tRNAs remains unclear. Although further studies are required to reveal the molecular mechanism, our results suggest that oxidative stress may be one of the reasons for this finding. Cdk5rap1 requires two [4Fe-4S] clusters for ms^2 group insertion (Forouhar et al., 2013); therefore, it is conceivable that ROS, such as H_2O_2 or $ONOO^-$, may oxidize these [4Fe-4S] clusters and inactivate Cdk5rap1. In support of our hypothesis, ROS-treated cells exhibited a rapid decrease in ms^2 modification that was effectively reversed by antioxidants. Thus, ROS generated by the mutation in mt-$tRNA^{Leu}$ might impair Cdk5RAP1-mediated ms^2 modification, which might further amplify mitochondrial dysfunction and ultimately accelerate myopathy in MELAS patients. In addition to mitochondrial disease, ms^2 modifications might be involved in a wide variety of human diseases in which ROS have been previously implicated, such as cardiac dysfunction and cancer (Schieber and Chandel, 2014).

In conclusion, this study reveals a unique quality control system in mitochondria by which the ms^2 modification of mt-tRNAs dynamically regulates mitochondrial protein synthesis and contributes to the development of myopathy in vivo. Our findings have important physiological implications for the basic mechanism of mitochondrial protein synthesis and provide insights into the pathological mechanism of mitochondrial disease.

EXPERIMENTAL PROCEDURES

Please see the Supplemental Experimental Procedures for additional details.

Animals

Cdk5rap1 KO mice were generated by crossing transgenic mice with exon 5 and 6 of *Cdk5rap1* floxed with LoxP sequence, with transgenic mice expressing Cre recombinase under the control of the CAG promoter. Mice were backcrossed to C57BL6/J mice for at least seven generations to eliminate Cre transgene and control genetic background. Littermates of WT and KO mice (8–12 weeks old) were used for experiments unless otherwise specified. Animals were housed at 25°C with 12 hr light and 12 hr dark cycles. A KD was purchased from Research Diets (D12369B). All animal procedures were approved by the Animal Ethics Committee of Kumamoto University (Approval ID, C25-163). Detailed information on genotyping can be found in the Supplemental Experimental Procedures.

Luciferase Assay

E. coli colonies were transformed with plasmids encoding dual *luciferase* for detecting decoding error, *GST-Cdk5rap1*, or dominant-negative *GST-Cdk5rap1*. Colonies were cultured at 37°C, and isopropyl β-D-1-thiogalactopyranoside (IPTG) was added to the cultures at a final concentration of 1 mM. After 1 hr of incubation, the cultures were harvested for the luciferase assay using the Dual-Luciferase Reporter Assay System (Promega). Detailed procedures for detecting decoding error can be found in the Supplemental Experimental Procedures.

Cell Culture and Transfection

Mammalian cells were grown in DMEM high-glucose medium (GIBCO) supplemented with 10% fetal bovine serum (FBS, HyClone) at 37°C and 5% CO_2. Transfection of the plasmid DNA was performed with Lipofectamine 2000 (Invitrogen).

Oxygen Consumption

The oxygen consumption rate in MEF cells and intact mitochondria was measured using an XF24 Analyzer (Seahorse Bioscience). The oxygen consumption rate was normalized to the total protein concentration for measurement in cells. Detailed procedures for the respiratory assay can be found in the Supplemental Experimental Procedures.

Gene Expression Assay

RNA was extracted from tissues using Trizol (Invitrogen) following the manufacturer's instructions. Quantitative PCR (qPCR) was performed using SYBR Premix Ex Taq (TAKARA). For examination of the expression levels of oxidative response genes, the results were normalized to the geometric mean of multiple reference genes (Hprt1, RPL13A, B2M, GAPDH, ACT). Then, a Z-transformation was applied to the results to calculate the *Z* score and construct a heatmap (Cheadle et al., 2003). The sequences of primers used can be found in the Supplemental Experimental Procedures.

Analysis of tRNA Modification

Total RNAs were isolated from bacteria and tissues using Trizol reagent (Invitrogen). RNA was digested with Nuclease P1 (Sigma) and subjected to mass spectrometry (Agilent 6460). For detecting tRNA modification using the qPCR-based method, we adapted a protocol described previously (Xie et al., 2013). Detailed procedures for the mass spectrometry and qPCR method can be found in the Supplemental Experimental Procedures. To measure the tRNA modification level in blood samples, blood samples were collected from MELAS patients using standard procedures approved by Kurume University (IRB#9715).

ATP Measurement

Small pieces of skeletal muscle and heart tissue were immediately dissected after sacrificing mice and snap frozen in liquid nitrogen until measurement. ATP was measured using the ATP Bioluminescence Assay Kit following the manufacturer's protocol (TA100, WAKO). The luminescence was measured using a Centro XS^3 LB960 (Berthold) and normalized to total protein concentration.

Cardiac Function Examination

Echocardiographs were examined in M-mode while the mice were under anesthesia using the Vevo2100 system (Fujifilm VisualSonics, Inc.) according to the manufacturer's instructions.

Statistical Analysis

Statistical analyses were performed using Prism 6 Software (GraphPad Software). An unpaired Student t test was used to test the differences between two groups. Analysis of variance (one-way ANOVA or two-way ANOVA) was used to test the difference among multiple groups followed by a post hoc examination of the p value between two groups. A two-tailed p value of 0.05 was considered statistically significant.

SUPPLEMENTAL INFORMATION

Supplemental Information includes seven figures and Supplemental Experimental Procedures and can be found with this article at http://dx.doi.org/10.1016/j.cmet.2015.01.019.

AUTHOR CONTRIBUTIONS

F.-Y.W. and K.T. designed the experiments and wrote the manuscript. F.-Y.W. and B.Z. performed the experiments. Takeo Suzuki and Tsutomu Suzuki performed the mass spectrometry experiments. H.H., K.M., and Y.O. performed cardiac examinations. Y.U. and S.M. performed TAC surgery and cardiac examinations. H. Michiue, A.F., and H. Matsui performed electron microscopy. Y.K. provided the blood samples. N.T., P.X., and T.K. performed the qPCR-based examination of tRNA modifications.

ACKNOWLEDGMENTS

We thank Nobuko Maeda for the technical assistance. This work was supported by a Grant-in-Aid for Scientific Research from the Ministry of Education, Culture, Sports, Science, and Technology of Japan, by the Japan Society for the Promotion of Science (JSPS) through its "Funding Program for Next Generation World-Leading Researchers," and by the Takeda Science Foundation.

Received: September 5, 2014
Revised: November 24, 2014
Accepted: January 26, 2015
Published: March 3, 2015

REFERENCES

Agris, P.F. (2004). Decoding the genome: a modified view. Nucleic Acids Res. *32*, 223–238.

Arragain, S., Handelman, S.K., Forouhar, F., Wei, F.Y., Tomizawa, K., Hunt, J.F., Douki, T., Fontecave, M., Mulliez, E., and Atta, M. (2010). Identification of eukaryotic and prokaryotic methylthiotransferase for biosynthesis of 2-methylthio-N^6-threonylcarbamoyladenosine in tRNA. J. Biol. Chem. *285*, 28425–28433.

Cheadle, C., Vawter, M.P., Freed, W.J., and Becker, K.G. (2003). Analysis of microarray data using Z score transformation. J. Mol. Diagn. *5*, 73–81.

Chen, Y., and Dorn, G.W., 2nd. (2013). PINK1-phosphorylated mitofusin 2 is a Parkin receptor for culling damaged mitochondria. Science *340*, 471–475.

Crimi, M., Bordoni, A., Menozzi, G., Riva, L., Fortunato, F., Galbiati, S., Del Bo, R., Pozzoli, U., Bresolin, N., and Comi, G.P. (2005). Skeletal muscle gene expression profiling in mitochondrial disorders. FASEB J. *19*, 866–868.

Dai, D.F., Hsieh, E.J., Liu, Y., Chen, T., Beyer, R.P., Chin, M.T., MacCoss, M.J., and Rabinovitch, P.S. (2012). Mitochondrial proteome remodelling in pressure overload-induced heart failure: the role of mitochondrial oxidative stress. Cardiovasc. Res. *93*, 79–88.

DiMauro, S., and Schon, E.A. (2003). Mitochondrial respiratory-chain diseases. N. Engl. J. Med. *348*, 2656–2668.

Durieux, J., Wolff, S., and Dillin, A. (2011). The cell-non-autonomous nature of electron transport chain-mediated longevity. Cell *144*, 79–91.

Forouhar, F., Arragain, S., Atta, M., Gambarelli, S., Mouesca, J.M., Hussain, M., Xiao, R., Kieffer-Jaquinod, S., Seetharaman, J., Acton, T.B., et al. (2013). Two Fe-S clusters catalyze sulfur insertion by radical-SAM methylthiotransferases. Nat. Chem. Biol. *9*, 333–338.

Grimsrud, P.A., Carson, J.J., Hebert, A.S., Hubler, S.L., Niemi, N.M., Bailey, D.J., Jochem, A., Stapleton, D.S., Keller, M.P., Westphall, M.S., et al. (2012). A quantitative map of the liver mitochondrial phosphoproteome reveals post-translational control of ketogenesis. Cell Metab. *16*, 672–683.

Hoshino, A., Mita, Y., Okawa, Y., Ariyoshi, M., Iwai-Kanai, E., Ueyama, T., Ikeda, K., Ogata, T., and Matoba, S. (2013). Cytosolic p53 inhibits Parkin-mediated mitophagy and promotes mitochondrial dysfunction in the mouse heart. Nat. Commun. *4*, 2308.

Houtkooper, R.H., Mouchiroud, L., Ryu, D., Moullan, N., Katsyuba, E., Knott, G., Williams, R.W., and Auwerx, J. (2013). Mitonuclear protein imbalance as a conserved longevity mechanism. Nature *497*, 451–457.

Ishikawa, K., Kimura, S., Kobayashi, A., Sato, T., Matsumoto, H., Ujiie, Y., Nakazato, K., Mitsugi, M., and Maruyama, Y. (2005). Increased reactive oxygen species and anti-oxidative response in mitochondrial cardiomyopathy. Circ. J. *69*, 617–620.

Jenner, L.B., Demeshkina, N., Yusupova, G., and Yusupov, M. (2010). Structural aspects of messenger RNA reading frame maintenance by the ribosome. Nat. Struct. Mol. Biol. *17*, 555–560.

Karamanlidis, G., Lee, C.F., Garcia-Menendez, L., Kolwicz, S.C., Jr., Suthammarak, W., Gong, G., Sedensky, M.M., Morgan, P.G., Wang, W., and Tian, R. (2013). Mitochondrial complex I deficiency increases protein acetylation and accelerates heart failure. Cell Metab. *18*, 239–250.

Kirino, Y., Yasukawa, T., Ohta, S., Akira, S., Ishihara, K., Watanabe, K., and Suzuki, T. (2004). Codon-specific translational defect caused by a wobble modification deficiency in mutant tRNA from a human mitochondrial disease. Proc. Natl. Acad. Sci. USA *101*, 15070–15075.

Kirino, Y., Goto, Y., Campos, Y., Arenas, J., and Suzuki, T. (2005). Specific correlation between the wobble modification deficiency in mutant tRNAs and the clinical features of a human mitochondrial disease. Proc. Natl. Acad. Sci. USA *102*, 7127–7132.

Kubli, D.A., and Gustafsson, Å.B. (2012). Mitochondria and mitophagy: the yin and yang of cell death control. Circ. Res. *111*, 1208–1221.

Laffel, L. (1999). Ketone bodies: a review of physiology, pathophysiology and application of monitoring to diabetes. Diabetes Metab. Res. Rev. *15*, 412–426.

Machnicka, M.A., Milanowska, K., Osman Oglou, O., Purta, E., Kurkowska, M., Olchowik, A., Januszewski, W., Kalinowski, S., Dunin-Horkawicz, S., Rother, K.M., et al. (2013). MODOMICS: a database of RNA modification pathways—2013 update. Nucleic Acids Res. *41* (Database issue), D262–D267.

Murphy, M.P. (2009). How mitochondria produce reactive oxygen species. Biochem. J. *417*, 1–13.

Reiter, V., Matschkal, D.M., Wagner, M., Globisch, D., Kneuttinger, A.C., Müller, M., and Carell, T. (2012). The CDK5 repressor CDK5RAP1 is a methylthiotransferase acting on nuclear and mitochondrial RNA. Nucleic Acids Res. *40*, 6235–6240.

Runkel, E.D., Liu, S., Baumeister, R., and Schulze, E. (2013). Surveillance-activated defenses block the ROS-induced mitochondrial unfolded protein response. PLoS Genet. *9*, e1003346.

Schieber, M., and Chandel, N.S. (2014). ROS function in redox signaling and oxidative stress. Curr. Biol. *24*, R453–R462.

Steinthorsdottir, V., Thorleifsson, G., Reynisdottir, I., Benediktsson, R., Jonsdottir, T., Walters, G.B., Styrkarsdottir, U., Gretarsdottir, S., Emilsson, V., Ghosh, S., et al. (2007). A variant in CDKAL1 influences insulin response and risk of type 2 diabetes. Nat. Genet. *39*, 770–775.

Suzuki, T. (2005). Biosynthesis and function of tRNA wobble modifications. Topics Curr. Genet. *12*, 24–69.

Suzuki, T., and Suzuki, T. (2014). A complete landscape of post-transcriptional modifications in mammalian mitochondrial tRNAs. Nucleic Acids Res. *42*, 7346–7357.

Suzuki, T., Suzuki, T., Wada, T., Saigo, K., and Watanabe, K. (2002). Taurine as a constituent of mitochondrial tRNAs: new insights into the functions of taurine and human mitochondrial diseases. EMBO J. *21*, 6581–6589.

Suzuki, T., Nagao, A., and Suzuki, T. (2011). Human mitochondrial tRNAs: biogenesis, function, structural aspects, and diseases. Annu. Rev. Genet. *45*, 299–329.

Torres, A.G., Batlle, E., and Ribas de Pouplana, L. (2014). Role of tRNA modifications in human diseases. Trends Mol. Med. *20*, 306–314.

Urbonavicius, J., Qian, Q., Durand, J.M., Hagervall, T.G., and Björk, G.R. (2001). Improvement of reading frame maintenance is a common function for several tRNA modifications. EMBO J. *20*, 4863–4873.

Wei, F.Y., Suzuki, T., Watanabe, S., Kimura, S., Kaitsuka, T., Fujimura, A., Matsui, H., Atta, M., Michiue, H., Fontecave, M., et al. (2011). Deficit of tRNA(Lys) modification by Cdkal1 causes the development of type 2 diabetes in mice. J. Clin. Invest. *121*, 3598–3608.

Wenz, T., Luca, C., Torraco, A., and Moraes, C.T. (2009). mTERF2 regulates oxidative phosphorylation by modulating mtDNA transcription. Cell Metab. *9*, 499–511.

Xie, P., Wei, F.Y., Hirata, S., Kaitsuka, T., Suzuki, T., Suzuki, T., and Tomizawa, K. (2013). Quantitative PCR measurement of tRNA 2-methylthio modification for assessing type 2 diabetes risk. Clin. Chem. *59*, 1604–1612.

Yasukawa, T., Suzuki, T., Ishii, N., Ohta, S., and Watanabe, K. (2001). Wobble modification defect in tRNA disturbs codon-anticodon interaction in a mitochondrial disease. EMBO J. *20*, 4794–4802.

Mitochondrion 20 (2015) 34–42

Contents lists available at ScienceDirect

Mitochondrion

journal homepage: www.elsevier.com/locate/mito

GDF15 is a novel biomarker to evaluate efficacy of pyruvate therapy for mitochondrial diseases

Yasunori Fujita [a], Masafumi Ito [a], Toshio Kojima [b], Shuichi Yatsuga [c], Yasutoshi Koga [c], Masashi Tanaka [d,*]

[a] Research Team for Mechanism of Aging, Tokyo Metropolitan Institute of Gerontology, 35-2 Sakae-cho, Itabashi, Tokyo 173-0015, Japan
[b] Health Support Center, Toyohashi University of Technology, 1-1 Hibarigaoka Tenpaku-cho, Toyohashi, Aichi 441-8580, Japan
[c] Department of Pediatrics and Child Health, Kurume University School of Medicine, 67 Asahi-machi, Kurume, Fukuoka 830-0011, Japan
[d] Department of Genomics for Longevity and Health, Tokyo Metropolitan Institute of Gerontology, 35-2 Sakae-cho, Itabashi, Tokyo 173-0015, Japan

ARTICLE INFO

Article history:
Received 20 May 2014
received in revised form 2 September 2014
accepted 29 October 2014
Available online 1 November 2014

Keywords:
GDF15
Pyruvate
Mitochondrial diseases
Cybrid
Microarray
Biomarker

ABSTRACT

Pyruvate therapy is a promising approach for the treatment of mitochondrial diseases. To identify novel biomarkers for diagnosis and to evaluate therapeutic efficacy, we performed microarray analysis of 2SD cybrid cells harboring a MELAS-causing mutation and control cells treated with either lactate or pyruvate. We found that expression and secretion of growth differentiation factor 15 (GDF15) were increased in 2SD cells treated with lactate and that serum GDF15 levels were significantly higher in patients with mitochondrial diseases than in those with other diseases, suggesting that GDF15 could be a useful marker for diagnosis and evaluating the therapeutic efficacy of pyruvate.

1. Introduction

Mitochondrial diseases are caused by mitochondrial or nuclear genome mutations that affect the functions of mitochondria. The symptoms are caused by impaired energy metabolism due to mitochondrial dysfunction and manifest mostly in tissues with a high energy demand such as brain, heart, and muscle. Mitochondrial myopathy, encephalopathy, lactic acidosis, and stroke-like episodes (MELAS) is one of the most common of the mitochondrial diseases (Pavlakis et al., 1984). The A-to-G transition at the 3243 position of the mitochondrial DNA (m.3243A > G) located in the mitochondrial $tRNA^{Leu\ (UUR)}$ gene is a MELAS-causing mutation, and it is detected in approximately 80% of patients with MELAS (Goto et al., 1990, 1992; Kirino et al., 2004; Yasukawa et al., 2000).

These pathogenic mutations typically result in defective ATP synthesis in mitochondria, and therefore ATP production depends on the glycolytic pathway. Since lactate production is aberrantly increased by the acceleration of glycolysis when energy demand is elevated, the lactate to pyruvate (L/P) ratio in serum is often increased in patients with mitochondrial diseases and has been clinically used for estimating the dysfunction of mitochondrial respiration. It is well known that the L/P ratio reflects the intracellular NADH/NAD^+ ratio. Since NAD^+ is indispensable for oxidation of glyceraldehyde 3-phosphate (GAP) to 1,3-bisphosphoglycerate (BPG) by glyceraldehyde 3-phosphate dehydrogenase (GAPDH) in the glycolytic pathway, a shortage of NAD^+ interrupts this reaction, resulting in decreased ATP biosynthesis. Tanaka et al. (2007) proposed that the addition of pyruvate would facilitate oxidation of NADH to NAD^+ via the lactate dehydrogenase reaction, which would restore ATP production by the glycolytic pathway even under defective respiratory conditions. Indeed, positive effects of sodium pyruvate on clinical manifestations of mitochondrial diseases have been reported (Koga et al., 2012; Saito et al., 2012). However, useful biomarkers for evaluating the therapeutic efficacy of pyruvate remain to be developed.

Cybrid cell lines established by the fusion of enucleated myoblast cells from a patient with a cultured cell line depleted of mtDNA have been used to elucidate the pathogenesis and underlying molecular mechanisms of mitochondrial diseases. We previously reported increased expression of amino acid starvation-responsive genes in cybrid cells with MELAS and NARP (neuropathy, ataxia, and retinitis pigmentosa) mutations (Fujita et al., 2007). In our earlier study (Kami et al., 2012), we found that exposure to excessive sodium lactate significantly increases the intracellular L/P and NADH/NAD^+ ratios in cybrid cells harboring the MELAS mutation (m.3243A > G), which implies worsening of lactic acidosis and NAD^+ shortage. On the other hand, we found that treatment with sodium pyruvate facilitates the ATP production and improves the energy status, as indicated by a decrease in the L/P ratio and retention of the NADH/NAD^+ ratio. Taken together, we considered that these experimental conditions would be ideal for identifying biomarker candidate genes, whose expression levels reflect

* Corresponding author. Tel.: +81 3 3964 3241; fax: +81 3 3579 4776.
E-mail address: mtanaka@tmig.or.jp (M. Tanaka).

http://dx.doi.org/10.1016/j.mito.2014.10.006
1567-7249/

the intracellular energy deficiency and the effect of pyruvate on energy metabolism.

In the present study, we performed a global gene expression analysis of cybrid cells with the MELAS mutation (m.3243A > G: 2SD cells) and control cybrid cells (2SA cells) treated or not with lactate or pyruvate. We identified several biomarker candidate genes, among which we focused on growth differentiation factor 15 (GDF15). The level of GDF15 in the conditioned medium was significantly higher in 2SD cells than in 2SA cells, which level was further increased by lactate but was not affected by pyruvate in 2SD cells. We also demonstrated that the concentration of GDF15 in the serum was markedly elevated in patients with mitochondrial diseases compared with that in those with other pediatric diseases. Thus, we identified GDF15 as a novel serum marker for the diagnosis of mitochondrial diseases and possibly for monitoring the disease status and progression and for evaluating the therapeutic efficacy of pyruvate.

2. Materials and methods

2.1. Cell culture

The 2SA and 2SD cybrid cell lines were previously established by Chomyn et al. (1992). Briefly, 14 cybrid clones were isolated after the fusion of enucleated myoblasts derived from a MELAS patient with mtDNA-deficient $\rho^0$206 cells generated from a human 143B osteosarcoma cell line. Among those clones, 10 clones had homoplasmic wild-type mtDNA, and 4 clones harbored strongly predominant mutant mtDNA. For our experiments, we chose two clones, 2SA and 2SD cybrid cell lines carrying 100% wild-type mtDNA and 94% m.3243A > G mutant mtDNA, respectively. The 2SD but not 2SA cybrid cells were shown to be defective in mitochondrial protein synthesis and respiratory capacity (Chomyn et al., 1992). Cells were cultured in high-glucose Dulbecco's modified Eagle's medium (DMEM) supplemented with 10% fetal bovine serum, 1 mM sodium pyruvate, and 0.4 mM uridine at 37 °C under a humidified atmosphere of 5% CO_2.

2.2. Microarray analysis

Total RNA was isolated from cells by using a miRNeasy mini kit (Qiagen, Venlo, Netherlands). One hundred nanograms of total RNA was labeled and amplified with a low input quick amp labeling kit (Agilent Technologies, Santa Clara, CA, USA) used according to the manufacturer's instructions. The labeled cRNA was hybridized to the Agilent SurePrint G3 Human GE 8x60K Microarray in a rotating hybridization oven at 10 rpm for 20 h at 65 °C. After hybridization, the microarrays were washed according to the manufacturer's instructions and scanned on an Agilent DNA Microarray Scanner with Scan Control software. The resulting images were processed, and raw data were collected by using Agilent Feature Extraction software. Expression data were analyzed by using GeneSpring GX 11 (Agilent Technologies). The signal intensity of each probe was normalized by a percentile shift, in which each value was divided by the 75th percentile of all values in its array. For pairwise comparison analysis, only the probes that had expression flags present under at least one condition were considered. The list was analyzed with Ingenuity Pathways Analysis software (Ingenuity Systems, Redwood, CA, USA)

2.3. Quantitative RT-PCR

Total RNA was reverse transcribed to cDNA with a High Capacity cDNA Reverse Transcription Kit (Life Technologies, Carlsbad, CA, USA) used according to the manufacturer's protocols. Real-time PCR was performed on the StepOnePlus Real-Time PCR System (Life Technologies) using Power SYBR Green PCR Master Mix. 18S rRNA gene was used as an internal control for normalization. The sequences of primers are listed in Supplementary Table 1.

2.4. Patients

A written informed consent was obtained from all patients or their legal guardians. Enrolled patients were diagnosed with mitochondrial diseases by medical doctors in Kurume University Hospital over the period of 2005–2013. Seventeen patients diagnosed at this hospital as having mitochondrial diseases were recruited for this study. As a control group, 13 patients diagnosed as having other pediatric diseases such as dwarfism were also recruited. The clinical information of the patients is listed in Supplementary Table 2. This study was approved by the Institutional Review Board (Kurume University #13099).

2.5. ELISA and multiplex suspension array

Cells were placed on 60-mm dishes 1 day before replacing the medium with fresh medium. Conditioned medium cultured for 24 h was collected, and the particulates were removed by centrifugation (at 500 ×g for 10 min, at 10,000 ×g for 30 min). The GDF15 and INHBE concentrations in the supernatants and in the sera of patients were determined in duplicate by using a Human GDF-15 Immunoassay (R&D Systems, Minneapolis, MN, USA) and enzyme-linked immunosorbent assay kit for Inhibin Beta E (Uscn Life Science, Wuhan, Hubei, PRC) according to the manufacturer's instructions. For measuring other cytokine concentrations, the sera were subjected to a multiplex suspension array, Bio-Plex Pro Human Cytokine Grp II Panel 21-Plex (Bio-Rad, Hercules, CA, USA). The cytokines measured by use of this array were the following: IL-1α, IL-2Rα, IL-3, IL-12 (p40), IL-16, IL-18, CTACK, GRO-α, HGF, IFN-α2, LIF, MCP-3, M-CSF, MIF, MIG, β-NGF, SCF, SCGF-β, SDF-1α, TNF-β, and TRAIL. We measured the FGF21 (BioVendor, Czech Republic) concentration in duplicate samples by ELISA. Unmeasurable high-concentration samples of FGF21 and GDF15 were diluted 10-fold prior to measurement. The value from each assay was determined by reference to the linear portion of the standard curves for FGF21 and GDF15. All assays were performed by a trained scientist or technical staff.

2.6. Statistical analysis

Statistical analyses were performed by using IBM SPSS statistics (IBM, Armonk, NY, USA). We used the nonparametric Mann–Whitney *U* test to validate differences in cytokine levels in serum between mitochondrial disease patients and controls. The correlation between GDF15 and FGF21 concentrations in serum was assessed by Spearman correlation analysis. We plotted the receiver operating characteristics (ROC) curve for GDF15, HGF, SCF, SCGF-β, and FGF21 and calculated the area under the curve (AUC). The data for the sensitivity and 100 minus the specificity were plotted on a continuous scale.

3. Results

3.1. Gene expression changes in response to intracellular energy deficiency in 2SD cells

We performed microarray analysis of 2SD cybrid cells harboring the MELAS mutation (m.3243A > G) and 2SA control cybrid cells treated with 10 mM lactate or 10 mM pyruvate for 0, 4 or 8 h (Fig. 1A). The numbers of gene probes whose signal intensities were altered by 2-fold for each comparison are given in Supplementary Tables 3–6. We found remarkable changes in gene expression in 2SD cells, but not in 2SA cells, treated with lactate for 8 h. As shown in Supplementary Fig. 1A, we then selected gene probes that were increased by lactate treatment for 8 h compared with those without treatment and concurrently up-regulated by lactate but not by pyruvate at 8 h after treatment and thereby identified 313 probes that were specifically up-regulated by lactate in 2SD cells at 8 h

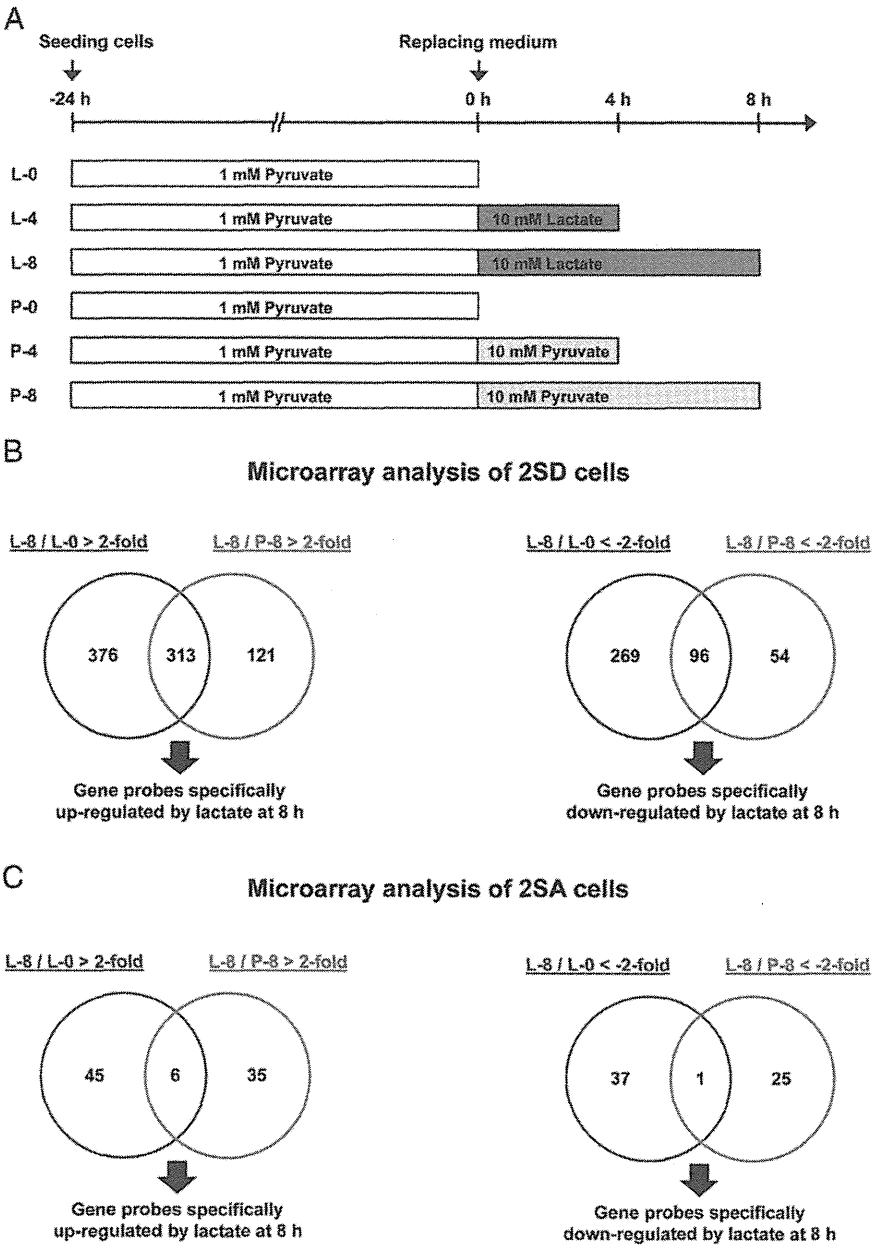

Fig. 1. Microarray analysis of 2SD and 2SA cells (A) Diagram of treatment protocols. Total RNA isolated from 2SD and 2SA cells treated with 10 mM lactate or 10 mM pyruvate for 0, 4, or 8 h were subjected to microarray analysis ($n = 2$). (B, C) Venn diagrams show the number of probes for genes in 2SD cells (B) or 2SA cells (C) that were increased (left panels) or decreased (right panels) in expression by lactate treatment for 8 h compared with their expression at 0 h and concurrently up-regulated by lactate but not by pyruvate after 8-h treatment. (For interpretation of the references to colour in this figure, the reader is referred to the web version of this article.)

(Fig. 1B). Using similar criteria (Supplementary Fig. 1B), we also identified 96 probes that were specifically down-regulated in 2SD cells by lactate treatment for 8 h (Fig. 1B). In 2SA cells, having normal mitochondrial function, the numbers of gene probes that responded to lactate treatment were limited (Fig. 1C). The clustering analysis of the 313 up-regulated (corresponding to 231 genes) and 96 down-regulated (corresponding to 75 genes) gene probes highlighted significant differences in gene expression patterns between 2SD and 2SA cells and also between lactate and pyruvate treatments (Fig. 2). These results suggest that a defective energy metabolism caused by exposure to a high dose of lactate resulted in significant changes in gene expression in 2SD cells.

3.2. Gene networks associated with intracellular energy deficiency in 2SD cells

In order to identify gene networks associated with a defective energy metabolism in the lactate-treated 2SD cells, a gene network analysis was performed on 231 up-regulated genes and 75 down-regulated ones. This analysis identified 11 and 5 gene networks for up- and down-regulated genes, respectively (Fig. 3 and Supplementary Figs. 2 and 3). The top-ranked gene network identified for the up-regulated genes contained those related to the amino-acid starvation response, such as ASNS, ATF3, NUPR1, DDIT3, CTH, TRIB3, STC2, and PCK2 (Fig. 3A). It is worth noting that GDF15, on which we focused in the

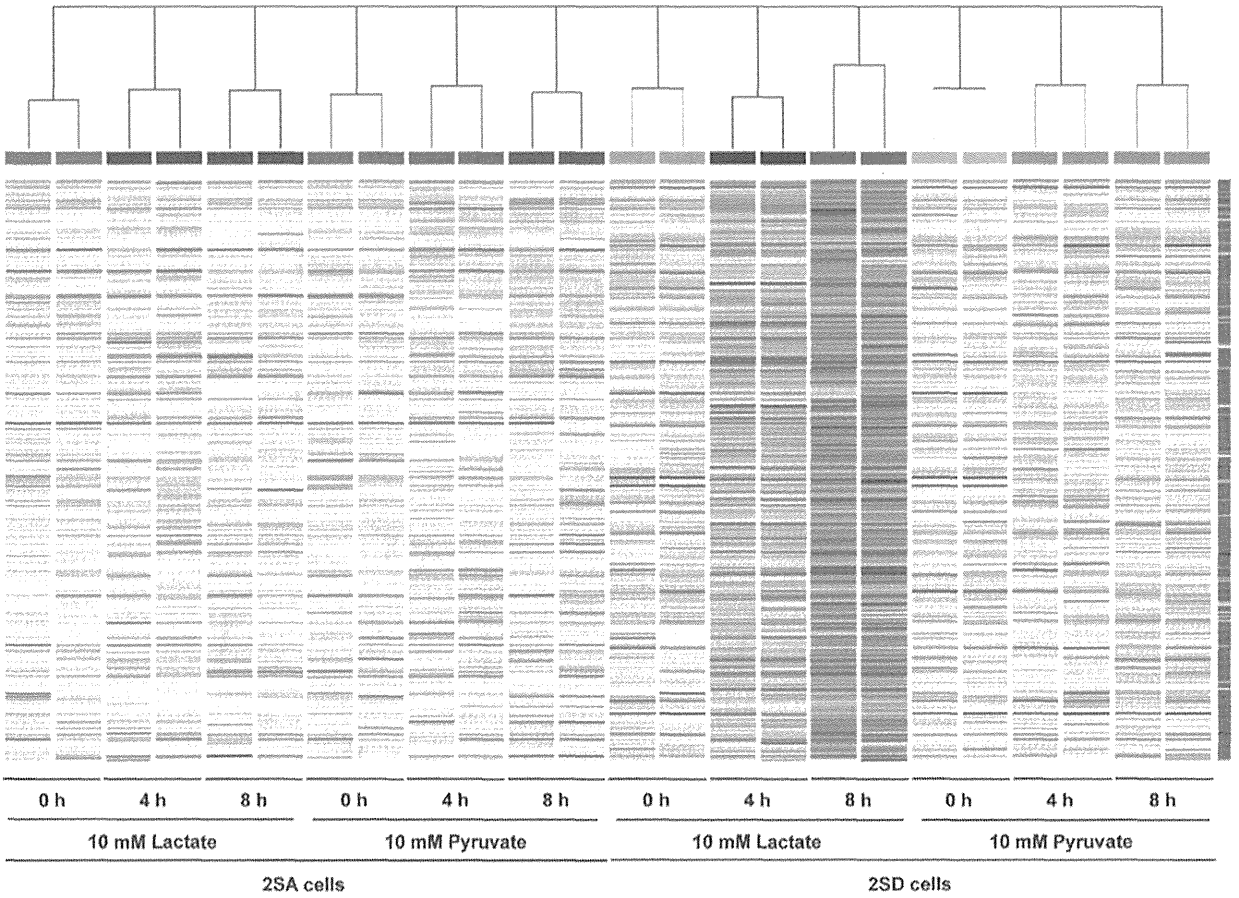

Fig. 2. Clustering analysis of the microarray data The gene probes up-regulated ($n = 313$) and down-regulated ($n = 96$) at 8 h after lactate treatment were subjected to clustering analysis. Part of the data are shown. (For interpretation of the references to colour in this figure, the reader is referred to the web version of this article.)

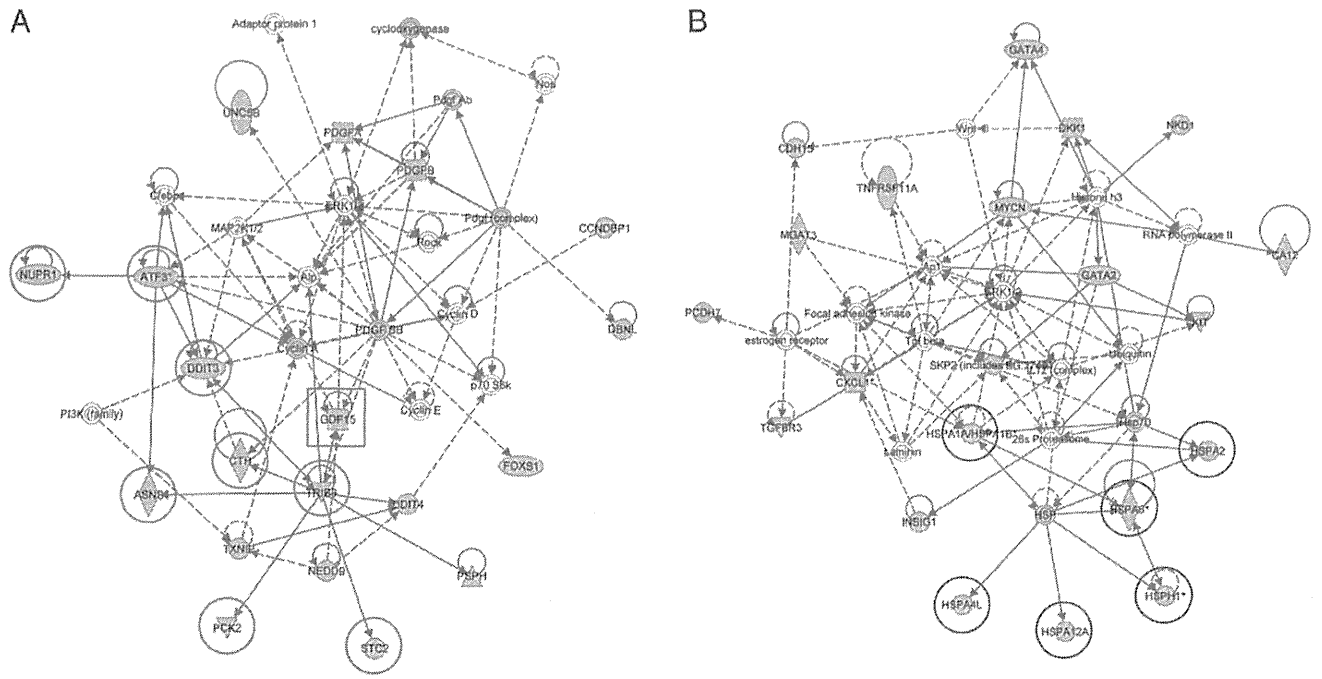

Fig. 3. Gene network analysis of the microarray data The genes specifically up-regulated ($n = 231$) and down-regulated ($n = 75$) at 8 h after lactate treatment were subjected to gene network analysis. The top-ranked gene networks in terms of the number of genes included are shown for up-regulated (A) and down-regulated (B) genes. Genes involved in the amino-acid starvation response (red circles) and heat-shock response (blue circles) as well as GDF15 (red square) are denoted. (For interpretation of the references to colour in this figure, the reader is referred to the web version of this article.)

present study, was included in this network. On the other hand, the gene network for down-regulated genes included those linked to the heat-shock protein response, such as HSPA1A, HSPA2, HSPA4L, HSPA8, HSPA12A, and HSPH1 (Fig. 3B).

3.3. GDF15 as a potential biomarker for diagnosis and evaluating the therapeutic efficacy of pyruvate

Proteins encoded by genes related to intracellular energy deficiency in 2SD cells and secreted into the medium could be potential biomarkers for mitochondrial diseases. Gene annotation analysis revealed the location of gene products that were specifically up- and down-regulated by lactate at 8 h (231 and 75 genes, respectively) (Table 1). Twenty-three up-regulated genes and 4 down-regulated genes were annotated to the extracellular space, each of which is listed in Tables 2 and 3. Among them, we focused on the top 2 ranked up-regulated genes, growth differentiation factor 15 (GDF15) and inhibin beta E (INHBE).

To validate the intracellular expression levels of these genes, we performed quantitative RT-PCR for GDF15 and INHBE. The expression levels of GDF15 (Fig. 4A) and INHBE (Fig. 4B) in the 2SD cells were increased by treatment with 10 mM lactate, but not with 10 mM pyruvate, for 4 or 8 h. Furthermore, GDF15 expression at 0 h was higher in 2SD cells than in 2SA cells. These results confirmed the reproducibility of our microarray data and identified GDF15 and INHBE as candidate biomarkers. To determine whether the secretion of GDF15 and INHBE proteins was increased in 2SD cells in response to lactate treatment, we measured their concentrations in medium from 2SA and 2SD cells cultured for 24 h in the presence of 1 mM pyruvate, 10 mM lactate, or 10 mM pyruvate. ELISA showed that the GDF15 levels were higher in the conditioned medium of 2SD cells than in that of 2SA cells under all of the culture conditions (Fig. 4C). Moreover, treatment with 10 mM lactate, but not with 10 mM pyruvate, promoted secretion of GDF15 in 2SD cells in comparison with treatment with 1 mM pyruvate, whereas 2SA cells did not respond to the high dose of lactate and pyruvate treatment. In contrast, INHBE protein was not detectable by ELISA in the conditioned medium of either 2SD or 2SA cells under any culture conditions (data not shown). These results indicate that GDF15 could be a potential biomarker for diagnosis and monitoring the disease status and progression as well as for assessing the therapeutic efficacy of pyruvate for the treatment of mitochondrial diseases.

3.4. GDF15 as a biomarker for diagnosis of mitochondrial diseases

In order to validate the feasibility of GDF15 as a serum biomarker, we measured its concentration in the serum of 17 patients with mitochondrial diseases as well as in that of 13 patients with other pediatric diseases as a control (Supplementary Table 2). ELISA showed that the average concentration of GDF15 in the serum of mitochondrial disease patients was 2632.9 pg/mL, whereas that for other pediatric disease patients was 285.2 pg/mL, suggesting that GDF15 levels were significantly increased in the serum of mitochondrial disease patients and could clearly distinguish mitochondrial disease patients from control patients (Fig. 5A).

Table 1
The location of probes (genes) up- and down-regulated in 2SD cells with lactate treatment for 8 h.

Location	Up-regulated		Down-regulated	
	Probe number	Gene number	Probe number	Gene number
Nucleus	39	35	14	14
Cytoplasm	51	47	25	19
Plasma membrane	37	33	16	16
Extracellular space	26	23	5	4
Unknown	160	93	36	22

Since fibroblast growth factor 21 (FGF21) was recently proposed as a diagnostic marker for mitochondrial diseases (Davis et al., 2013; Suomalainen et al., 2011), we also measured the FGF21 levels in the serum of the same mitochondrial disease patients and control patients (Fig. 5B). The serum FGF21 levels were higher in patients with mitochondrial diseases than in those with other diseases. Furthermore, there was a good correlation between the serum GDF15 and FGF21 levels (Fig. 5C).

In an attempt to find additional biomarkers, we determined the serum levels of 21 cytokines in the same patients by using the multiplex suspension array. As shown in Supplementary Fig. 4A, the serum concentrations of HGF and SCF were higher in patients with mitochondrial diseases than in control patients, whereas the serum levels of SCGF-β were lower in the former than in the latter.

Finally, we performed ROC curve analysis of GDF15, HGF, SCF, SCGF-β, and FGF21. As shown in Fig. 5D, the area under the curves (AUC) for GDF15 (0.986) was higher than that for FGF21 (0.787). The AUC for FGF21 was similar to those for HGF (0.747), SCF (0.729), and SCGF-β (0.837) (Supplementary Fig. 4B), indicating that GDF15 had the maximum sensitivity and specificity for diagnosis of mitochondrial diseases. These results suggest that GDF15 has the greatest potential as a novel diagnostic marker for MELAS and other mitochondrial diseases.

4. Discussion

Based on the global gene expression analysis of cybrid cells with mitochondrial dysfunction, we identified GDF15 as a potential biomarker whose expression and secretion reflected the intracellular energy deficiency and the effect of pyruvate therapy on the energy metabolism. We then determined the serum levels of GDF15 in patients with mitochondrial diseases and other diseases and identified GDF15 as a novel diagnostic marker for mitochondrial diseases. Although additional clinical studies are needed, the serum GDF15 concentration may be a useful biomarker not only for diagnosis of mitochondrial diseases but also for monitoring the disease status and progression as well as for determining the efficacy of pyruvate therapy.

GDF15 is a member of the transforming growth factor-β (TGF-β) superfamily and is widely expressed in mammalian tissues (Unsicker et al., 2013). GDF15 plays important roles in multiple pathologies including cardiovascular diseases, cancer, and inflammation. It has been shown that GDF15 is up-regulated by tumor suppressor p53 in response to high glucose or treatment with anti-cancer compounds (Baek et al., 2002; Li et al., 2013; Yang et al., 2003). The p53 protein is a transcription factor that responds to a variety of stresses such as DNA damage, oxidative stress, hypoxia, and metabolic stress, and it activates the expression of genes to induce cell cycle arrest, DNA repair, senescence, and cell death (Sermeus and Michiels, 2011; Sperka et al., 2012; Zhang et al., 2010). CDKN1A (p21), a potent cyclin-dependent kinase inhibitor, is a major downstream effector of p53, which induces cell-cycle arrest (Sperka et al., 2012). In our microarray data, the CDKN1A expression level was 3.5-fold increased by lactate treatment of 2SD cells (data not shown). Previous reports demonstrated increased expression of CDKN1A in the skeletal muscle of patients with mitochondrial diseases and a cell line depleted of mitochondrial DNA (Behan et al., 2005; Crimi et al., 2005). Besides CDKN1A, we found other p53 effector genes in the list of genes up-regulated in the lactate-treated 2SD cells, including GADD45A, EGR2, DDIT3, CHMP4C, SESN2, ULBP1, DDIT4, and NUPR1 (data not shown). These results suggest that p53 activation may have played an important role in the induction of GDF15 expression in 2SD cells treated with lactate. It has been also demonstrated that p53 activation caused by metabolic stress is mediated by AMP-activated protein kinase (AMPK; Zhang et al., 2010). Our previous metabolomic profiling revealed that the ATP level drops but that the ADP and AMP levels are increased in lactate-treated 2SD cells (Kami et al., 2012), implying that elevation of the AMP/ATP ratio may activate p53 through AMPK activation. Taken together, it is possible that p53 induced GDF15 expression in

Table 2
Genes annotated to the extracellular space among those specifically up-regulated by lactate treatment for 8 h.

Gene symbol	Accession number	Entrez gene name	Fold change	
			L-8/L-0[a]	L-8/P-8[b]
GDF15	NM_004864	Growth differentiation factor 15	27.4	14.8
INHBE	NM_031479	Inhibin, beta E	15.0	9.4
AREG	NM_001657	Amphiregulin	14.0	2.2
ECM2	NM_001393	Extracellular matrix protein 2, female organ and adipocyte specific	11.8	9.0
ADM2	NM_024866	Adrenomedullin 2	10.3	3.0
MMP3	NM_002422	Matrix metallopeptidase 3 (stromelysin 1, progelatinase)	9.8	4.2
IL1A	NM_000575	Interleukin 1, alpha	7.6	6.0
C12orf39	ENST00000256969	Chromosome 12 open reading frame 39	6.3	6.7
APOL6	NM_030641	Apolipoprotein L, 6	6.2	3.8
SCG5	NM_003020	Secretogranin V (7B2 protein)	5.2	3.0
SPOCK2	NM_014767	Sparc/osteonectin, cwcv and kazal-like domains proteoglycan (testican) 2	5.1	6.6
AMTN	NM_212557	Amelotin	5.0	3.9
IL23A	NM_016584	Interleukin 23, alpha subunit p19	4.4	2.8
ADAMTS17	NM_139057	ADAM metallopeptidase with thrombospondin type 1 motif, 17	3.5	2.2
VEGFA	NM_001025370	Vascular endothelial growth factor A	3.4	2.5
STC2	NM_003714	Stanniocalcin 2	3.4	2.6
PDGFB	NM_002608	Platelet-derived growth factor beta polypeptide	2.8	3.8
C1QTNF1	NM_198594	C1q and tumor necrosis factor related protein 1	2.6	2.9
HECW2	NM_020760	HECT, C2 and WW domain containing E3 ubiquitin protein ligase 2	2.4	2.1
IGFALS	NM_004970	Insulin-like growth factor binding protein, acid labile subunit	2.3	2.5
IGFBP1	NM_000596	Insulin-like growth factor binding protein 1	2.3	2.1
PDGFA	NM_002607	Platelet-derived growth factor alpha polypeptide	2.2	2.2
CLEC3B	NM_003278	C-type lectin domain family 3, member B	2.1	2.2

[a]Fold change between 8 h and 0 h after lactate treatment
[b]Fold change between lactate treatment and pyruvate treatment at 8 h

response to AMPK activation caused by the intracellular energy deficiency. However, it remains to be determined whether other stresses such as oxidative stress may also have participated in p53 activation and GDF15 induction in the lactate-treated 2SD cells.

Gene network analysis demonstrated that the top-ranked network contained not only genes associated with the amino-acid starvation response but also the GDF15 gene (Fig. 3A). In a mouse model of late-onset mitochondrial myopathy, the expression of amino-acid starvation-responsive genes was shown to be elevated (Tyynismaa et al., 2010). The asparagine synthetase (ASNS), which is a representative gene involved in the amino-acid starvation response, has been reported to be up-regulated in the skeletal muscle of patients with mitochondrial diseases and in cybrid cells established from a mitochondrial disease patient (Crimi et al., 2005; Fujita et al., 2007). Activating transcription factor 4 (ATF4) is a master regulator of integrated stress responses (ISR), in which a variety of stresses, including amino-acid starvation as well as glucose starvation, ER stress, hypoxia, and oxidative stress, induce phosphorylation of eIF2α followed by up-regulation of ATF4 to activate expression of stress-responsive genes (Harding et al., 2003; Jiang et al., 2004; Rouschop et al., 2010; Rzymski et al., 2010; Teske et al., 2011). It is noteworthy to point out that GDF15 has been shown to be up-regulated by ATF4 in mouse embryonic fibroblasts (Jousse et al., 2007). Taken together, such findings suggest that the ISR pathway may also contribute to the induction of GDF15 in response to defective energy metabolism and play a role in the pathogenesis of mitochondrial diseases.

In the present study, we validated the clinical usefulness of GDF15 as a diagnostic marker by determining the serum GDF15 levels in patients with mitochondrial diseases and in those with other pediatric diseases. The results showed that serum GDF15 levels were significantly elevated in patients with mitochondrial diseases, which finding is consistent with a recent report (Kalko et al., 2014). We also demonstrated that GDF15 had higher sensitivity and specificity than FGF21, which was recently identified as a sensitive and specific blood biomarker for muscle pathology in a wide range of mitochondrial diseases in adults and children (Suomalainen et al., 2011). Our small-scale study, however, may have underestimated the clinical usefulness of FGF21, because the AUC for FGF21 reported by 2 independent groups (0.95 and 0.91) was higher than that in the present study (0.787).

Using the multiplex suspension array, we also identified HGF, SCF, and SCGF-β as potential diagnostic markers for mitochondrial diseases. The ROC curve analysis, however, revealed that GDF15 had the maximum sensitivity and specificity for diagnosis of mitochondrial diseases compared with HGF, SCF, SCGF-β, or FGF21. Based on the microarray analysis, we also selected INHBE as the next best candidate gene (Table 2). INHBE is a member of the activin beta family, which has been reported to be primarily expressed in the liver and up-regulated by drug-induced ER stress, cysteine deprivation, and insulin treatment (Bruning et al., 2012; Dombroski et al., 2010; Hashimoto et al., 2009; Lee et al., 2008). Although secreted INHBE protein was not detectable in the conditioned medium from the cell cultures, we are currently investigating the clinical usefulness of INHBE as a biomarker for diagnosis and monitoring of the disease status and progression.

Table 3
Genes annotated to the extracellular space among those specifically down-regulated by lactate treatment for 8 h.

Gene symbol	Accession number	Entrez gene name	Fold change	
			L-8/L-0[a]	L-8/P-8[b]
CXCL1	NM_001511	Chemokine (C-X-C motif) ligand 1 (melanoma growth stimulating activity, alpha)	−3.4	−2.6
PDZRN3	NM_015009	PDZ domain containing ring finger 3	−2.4	−2.0
SLC39A10	NM_020342	Solute carrier family 39 (zinc transporter), member 10	−2.3	−2.9
DKK1	NM_012242	Dickkopf 1 homolog (Xenopus laevis)	−2.1	−2.3

[a]Fold change between 8 h and 0 h after lactate treatment
[b]Fold change between lactate treatment and pyruvate treatment at 8 h

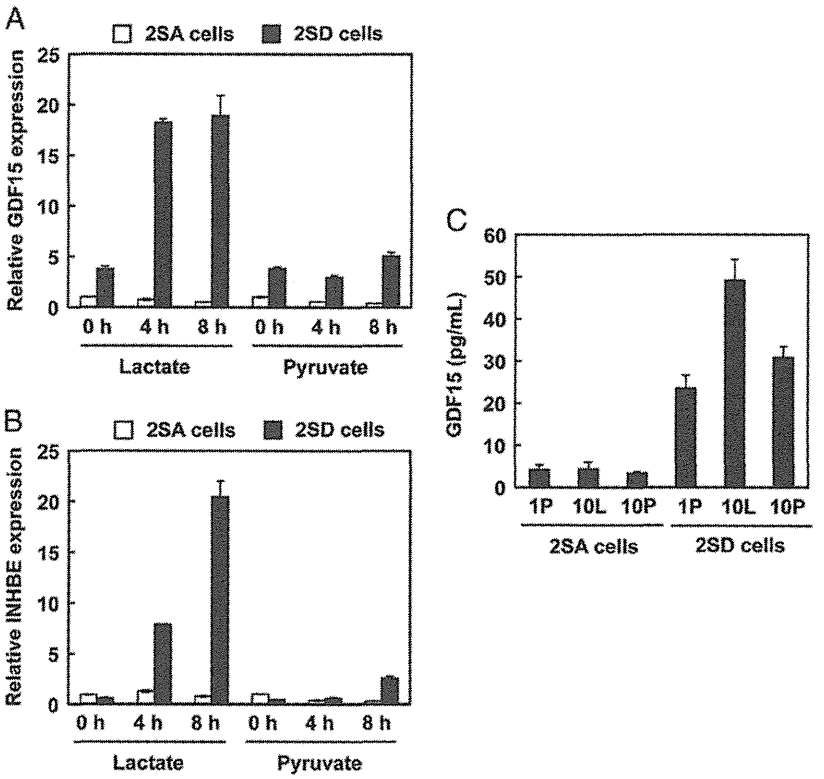

Fig. 4. Quantitative RT-PCR and ELISA for GDF15 and INHBE Total RNA isolated from 2SA and 2SD cells treated with 10 mM lactate or 10 mM pyruvate for 0, 4 or 8 h (n = 3) were subjected to quantitative RT-PCR for GDF15 (A) and INHBE (B). (C) The conditioned medium collected from 2SA and 2SD cell cultures treated with 10 mM lactate (10 L), 10 mM pyruvate (10P) or 1 mM pyruvate (1P) for 24 h was subjected to ELISA for GDF15 protein ($n = 3$).

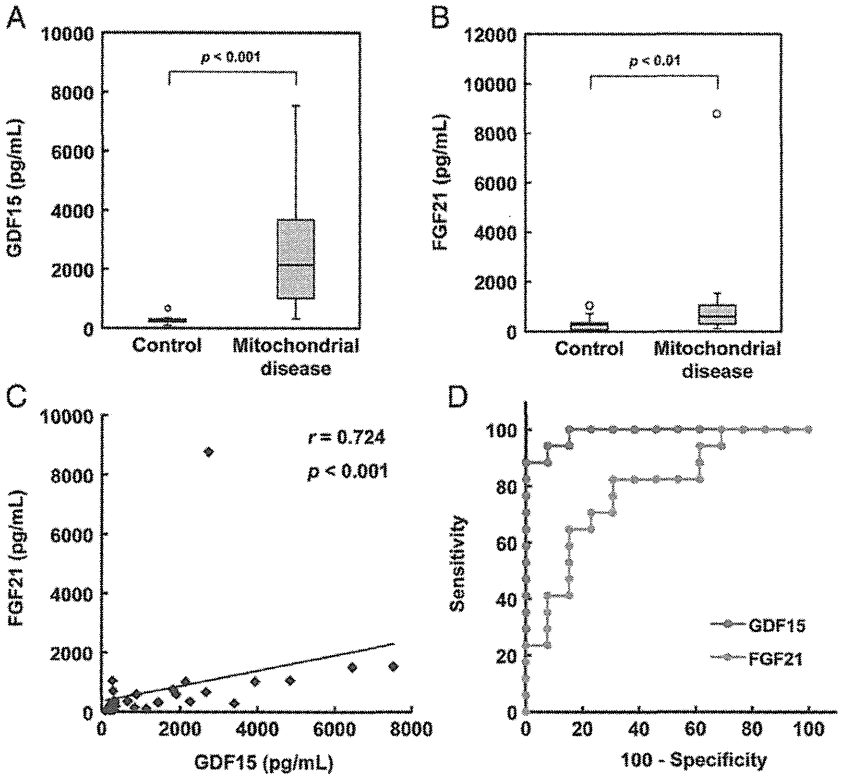

Fig. 5. Measurement of the GDF15 and FGF21 concentrations in the serum of patients. The serum GDF15 (A) and FGF21 (B) concentrations in 17 patients with mitochondrial diseases as well as those in 13 patients with other pediatric diseases were determined by ELISA. The outlier is shown with an open symbol. (C) A correlation analysis between the serum GDF15 and FGF21 levels was performed for the patients described above by use of IBM SPSS statistics. (D) The ROC curve analysis for GDF15 and FGF21 was performed. Areas under the curves (AUC) for GDF15 and FGF21 were 0.986 (95% CI 0.957-1.000) and 0.787 (95% CI 0.621-0.953), respectively.

It is well known that mitochondrial dysfunction is associated with the pathology of various diseases such as Parkinson's disease, Alzheimer's disease, diabetes, and aging (Exner et al., 2012; Lopez-Otin et al., 2013; Martin and McGee, 2014). GDF15, which may reflect mitochondria dysfunction, could be a useful marker for those diseases and the aging process. In support of this idea, the serum GDF15 level was reported to be elevated under various pathological conditions such as cancers, cardiovascular diseases, diabetes, and obesity (Dostalova et al., 2009; Kempf et al., 2007; Welsh et al., 2003); however, in most cases, it was not as high as that observed in mitochondrial diseases. Recent cohort studies also demonstrated that the serum GDF15 level is a novel predictor of all-cause mortality and is associated with cognitive performance and cognitive decline (Fuchs et al., 2013; Wiklund et al., 2010). We thus anticipate that GDF15 will attract more interest with respect to a variety of diseases and aging associated with mitochondrial dysfunction.

In conclusion, we identified GDF15 as a novel serum marker for the diagnosis of mitochondrial diseases and possibly both for monitoring the disease status and progression and for evaluating the therapeutic efficacy of pyruvate. Large-scale clinical trials including combined use of other markers such as FGF21 should confirm the clinical usefulness of GDF15.

Acknowledgments

This study was supported in part by the Ministry of Education, Culture, Sports, Science, and Technology of Japan; GMEXT/JSPS KAKENHI Grant Number: A-25242062, A-22240072, B-21390459, C-26670481, C-21590411, CER-24650414 (to M.T.), C-26350922 (to Y.F.), C-25461571 (to Y.K.), and YSB-25860891 (to S.Y.); the Ministry of Health, Labor, and Welfare of Japan; Grants-in-Aid for Research on Intractable Diseases (Mitochondrial Disorders): 23-Nanchi-Ippan-016, 23-Nanchi-Ippan-116, and 24-Nanchi-Ippan-005 (to M.T., and Y.K.); and the Takeda Science Foundation (to M.T.).

Appendix A. Supplementary data

Supplementary data to this article can be found online at http://dx.doi.org/10.1016/j.mito.2014.10.006.

References

Baek, S.J., Wilson, L.C., Eling, T.E., 2002. Resveratrol enhances the expression of non-steroidal anti-inflammatory drug-activated gene (NAG-1) by increasing the expression of p53. Carcinogenesis 23, 425–434.

Behan, A., Doyle, S., Farrell, M., 2005. Adaptive responses to mitochondrial dysfunction in the rho degrees Namalwa cell. Mitochondrion 5, 173–193.

Bruning, A., Matsingou, C., Brem, G.J., Rahmeh, M., Mylonas, I., 2012. Inhibin beta E is up-regulated by drug-induced endoplasmic reticulum stress as a transcriptional target gene of ATF4. Toxicol. Appl. Pharmacol. 264, 300–304.

Chomyn, A., Martinuzzi, A., Yoneda, M., Daga, A., Hurko, O., Johns, D., Lai, S.T., Nonaka, I., Angelini, C., Attardi, G., 1992. MELAS mutation in mtDNA binding site for transcription termination factor causes defects in protein synthesis and in respiration but no change in levels of upstream and downstream mature transcripts. Proc. Natl. Acad. Sci. U. S. A. 89, 4221–4225.

Crimi, M., Bordoni, A., Menozzi, G., Riva, L., Fortunato, F., Galbiati, S., Del Bo, R., Pozzoli, U., Bresolin, N., Comi, G.P., 2005. Skeletal muscle gene expression profiling in mitochondrial disorders. Faseb J. 19, 866–868.

Davis, R.L., Liang, C., Edema-Hildebrand, F., Riley, C., Needham, M., Sue, C.M., 2013. Fibroblast growth factor 21 is a sensitive biomarker of mitochondrial disease. Neurology 81, 1819–1826.

Dombroski, B.A., Nayak, R.R., Ewens, K.G., Ankener, W., Cheung, V.G., Spielman, R.S., 2010. Gene expression and genetic variation in response to endoplasmic reticulum stress in human cells. Am. J. Hum. Genet. 86, 719–729.

Dostalova, I., Roubicek, T., Bartlova, M., Mraz, M., Lacinova, Z., Haluzikova, D., Kavalkova, P., Matoulek, M., Kasalicky, M., Haluzik, M., 2009. Increased serum concentrations of macrophage inhibitory cytokine-1 in patients with obesity and type 2 diabetes mellitus: the influence of very low calorie diet. Eur. J. Endocrinol. 161, 397–404.

Exner, N., Lutz, A.K., Haass, C., Winklhofer, K.F., 2012. Mitochondrial dysfunction in Parkinson's disease: molecular mechanisms and pathophysiological consequences. EMBO J. 31, 3038–3062.

Fuchs, T., Trollor, J.N., Crawford, J., Brown, D.A., Baune, B.T., Samaras, K., Campbell, L., Breit, S.N., Brodaty, H., Sachdev, P., Smith, E., 2013. Macrophage inhibitory cytokine-1 is associated with cognitive impairment and predicts cognitive decline - the Sydney Memory and Aging Study. Aging Cell 12, 882–889.

Fujita, Y., Ito, M., Nozawa, Y., Yoneda, M., Oshida, Y., Tanaka, M., 2007. CHOP (C/EBP homologous protein) and ASNS (asparagine synthetase) induction in cybrid cells harboring MELAS and NARP mitochondrial DNA mutations. Mitochondrion 7, 80–88.

Goto, Y., Nonaka, I., Horai, S., 1990. A mutation in the tRNA(Leu)(UUR) gene associated with the MELAS subgroup of mitochondrial encephalomyopathies. Nature 348, 651–653.

Goto, Y., Horai, S., Matsuoka, T., Koga, Y., Nihei, K., Kobayashi, M., Nonaka, I., 1992. Mitochondrial myopathy, encephalopathy, lactic acidosis, and stroke-like episodes (MELAS): a correlative study of the clinical features and mitochondrial DNA mutation. Neurology 42, 545–550.

Harding, H.P., Zhang, Y., Zeng, H., Novoa, I., Lu, P.D., Calfon, M., Sadri, N., Yun, C., Popko, B., Paules, R., Stojdl, D.F., Bell, J.C., Hettmann, T., Leiden, J.M., Ron, D., 2003. An integrated stress response regulates amino acid metabolism and resistance to oxidative stress. Mol. Cell 11, 619–633.

Hashimoto, O., Sekiyama, K., Matsuo, T., Hasegawa, Y., 2009. Implication of activin E in glucose metabolism: transcriptional regulation of the inhibin/activin betaE subunit gene in the liver. Life Sci. 85, 534–540.

Jiang, H.Y., Wek, S.A., McGrath, B.C., Lu, D., Hai, T., Harding, H.P., Wang, X., Ron, D., Cavener, D.R., Wek, R.C., 2004. Activating transcription factor 3 is integral to the eukaryotic initiation factor 2 kinase stress response. Mol. Cell. Biol. 24, 1365–1377.

Jousse, C., Deval, C., Maurin, A.C., Parry, L., Cherasse, Y., Chaveroux, C., Lefloch, R., Lenormand, P., Bruhat, A., Fafournoux, P., 2007. TRB3 inhibits the transcriptional activation of stress-regulated genes by a negative feedback on the ATF4 pathway. J. Biol. Chem. 282, 15851–15861.

Kalko, S.G., Paco, S., Jou, C., Rodriguez, M.A., Meznaric, M., Rogac, M., Jekovec-Vrhovsek, M., Sciacco, M., Moggio, M., Fagiolari, G., De Paepe, B., De Meirleir, L., Ferrer, I., Roig-Quilis, M., Munell, F., Montoya, J., Lopez-Gallardo, E., Ruiz-Pesini, E., Artuch, R., Montero, R., Torner, F., Nascimento, A., Ortez, C., Colomer, J., Jimenez-Mallebrera, C., 2014. Transcriptomic profiling of TK2 deficient human skeletal muscle suggests a role for the p53 signalling pathway and identifies growth and differentiation factor-15 as a potential novel biomarker for mitochondrial myopathies. BMC Genomics 15, 91.

Kami, K., Fujita, Y., Igarashi, S., Koike, S., Sugawara, S., Ikeda, S., Sato, N., Ito, M., Tanaka, M., Tomita, M., Soga, T., 2012. Metabolomic profiling rationalized pyruvate efficacy in cybrid cells harboring MELAS mitochondrial DNA mutations. Mitochondrion 12, 644–653.

Kempf, T., Horn-Wichmann, R., Brabant, G., Peter, T., Allhoff, T., Klein, G., Drexler, H., Johnston, N., Wallentin, L., Wollert, K.C., 2007. Circulating concentrations of growth-differentiation factor 15 in apparently healthy elderly individuals and patients with chronic heart failure as assessed by a new immunoradiometric sandwich assay. Clin. Chem. 53, 284–291.

Kirino, Y., Yasukawa, T., Ohta, S., Akira, S., Ishihara, K., Watanabe, K., Suzuki, T., 2004. Codon-specific translational defect caused by a wobble modification deficiency in mutant tRNA from a human mitochondrial disease. Proc. Natl. Acad. Sci. U. S. A. 101, 15070–15075.

Koga, Y., Povalko, N., Katayama, K., Kakimoto, N., Matsuishi, T., Naito, E., Tanaka, M., 2012. Beneficial effect of pyruvate therapy on Leigh syndrome due to a novel mutation in PDH E1alpha gene. Brain Dev. 34, 87–91.

Lee, J.I., Dominy Jr., J.E., Sikalidis, A.K., Hirschberger, L.L., Wang, W., Stipanuk, M.H., 2008. HepG2/C3A cells respond to cysteine deprivation by induction of the amino acid deprivation/integrated stress response pathway. Physiol. Genomics 33, 218–229.

Li, J., Yang, L., Qin, W., Zhang, G., Yuan, J., Wang, F., 2013. Adaptive induction of growth differentiation factor 15 attenuates endothelial cell apoptosis in response to high glucose stimulus. PLoS One 8, e65549.

Lopez-Otin, C., Blasco, M.A., Partridge, L., Serrano, M., Kroemer, G., 2013. The hallmarks of aging. Cell 153, 1194–1217.

Martin, S.D., McGee, S.L., 2014. The role of mitochondria in the aetiology of insulin resistance and type 2 diabetes. Biochim. Biophys. Acta 1840, 1303–1312.

Pavlakis, S.G., Phillips, P.C., DiMauro, S., De Vivo, D.C., Rowland, L.P., 1984. Mitochondrial myopathy, encephalopathy, lactic acidosis, and strokelike episodes: a distinctive clinical syndrome. Ann. Neurol. 16, 481–488.

Rouschop, K.M., van den Beucken, T., Dubois, L., Niessen, H., Bussink, J., Savelkouls, K., Keulers, T., Mujcic, H., Landuyt, W., Voncken, J.W., Lambin, P., van der Kogel, A.J., Koritzinsky, M., Wouters, B.G., 2010. The unfolded protein response protects human tumor cells during hypoxia through regulation of the autophagy genes MAP1LC3B and ATG5. J. Clin. Invest. 120, 127–141.

Rzymski, T., Milani, M., Pike, L., Buffa, F., Mellor, H.R., Winchester, L., Pires, I., Hammond, E., Ragoussis, I., Harris, A.L., 2010. Regulation of autophagy by ATF4 in response to severe hypoxia. Oncogene 29, 4424–4435.

Saito, K., Kimura, N., Oda, N., Shimomura, H., Kumada, T., Miyajima, T., Murayama, K., Tanaka, M., Fujii, T., 2012. Pyruvate therapy for mitochondrial DNA depletion syndrome. Biochim. Biophys. Acta 1820, 632–636.

Sermeus, A., Michiels, C., 2011. Reciprocal influence of the p53 and the hypoxic pathways. Cell Death Dis. 2, e164.

Sperka, T., Wang, J., Rudolph, K.L., 2012. DNA damage checkpoints in stem cells, ageing and cancer. Nat. Rev. Mol. Cell Biol. 13, 579–590.

Suomalainen, A., Elo, J.M., Pietilainen, K.H., Hakonen, A.H., Sevastianova, K., Korpela, M., Isohanni, P., Marjavaara, S.K., Tyni, T., Kiuru-Enari, S., Pihko, H., Darin, N., Ounap, K., Kluijtmans, L.A., Paetau, A., Buzkova, J., Bindoff, L.A., Annunen-Rasila, J., Uusimaa, J., Rissanen, A., Yki-Jarvinen, H., Hirano, M., Tulinius, M., Smeitink, J., Tyynismaa, H., 2011. FGF-21 as a biomarker for muscle-manifesting mitochondrial respiratory chain deficiencies: a diagnostic study. Lancet Neurol. 10, 806–818.

Tanaka, M., Nishigaki, Y., Fuku, N., Ibi, T., Sahashi, K., Koga, Y., 2007. Therapeutic potential of pyruvate therapy for mitochondrial diseases. Mitochondrion 7, 399–401.

Teske, B.F., Wek, S.A., Bunpo, P., Cundiff, J.K., McClintick, J.N., Anthony, T.G., Wek, R.C., 2011. The eIF2 kinase PERK and the integrated stress response facilitate activation of ATF6 during endoplasmic reticulum stress. Mol. Biol. Cell 22, 4390–4405.

Tyynismaa, H., Carroll, C.J., Raimundo, N., Ahola-Erkkila, S., Wenz, T., Ruhanen, H., Guse, K., Hemminki, A., Peltola-Mjosund, K.E., Tulkki, V., Oresic, M., Moraes, C.T., Pietilainen, K., Hovatta, I., Suomalainen, A., 2010. Mitochondrial myopathy induces a starvation-like response. Hum. Mol. Genet. 19, 3948–3958.

Unsicker, K., Spittau, B., Krieglstein, K., 2013. The multiple facets of the TGF-beta family cytokine growth/differentiation factor-15/macrophage inhibitory cytokine-1. Cytokine Growth Factor Rev. 24, 373–384.

Welsh, J.B., Sapinoso, L.M., Kern, S.G., Brown, D.A., Liu, T., Bauskin, A.R., Ward, R.L., Hawkins, N.J., Quinn, D.I., Russell, P.J., Sutherland, R.L., Breit, S.N., Moskaluk, C.A., Frierson Jr., H.F., Hampton, G.M., 2003. Large-scale delineation of secreted protein biomarkers overexpressed in cancer tissue and serum. Proc. Natl. Acad. Sci. U. S. A. 100, 3410–3415.

Wiklund, F.E., Bennet, A.M., Magnusson, P.K., Eriksson, U.K., Lindmark, F., Wu, L., Yaghoutyfam, N., Marquis, C.P., Stattin, P., Pedersen, N.L., Adami, H.O., Gronberg, H., Breit, S.N., Brown, D.A., 2010. Macrophage inhibitory cytokine-1 (MIC-1/GDF15): a new marker of all-cause mortality. Aging Cell 9, 1057–1064.

Yang, H., Filipovic, Z., Brown, D., Breit, S.N., Vassilev, L.T., 2003. Macrophage inhibitory cytokine-1: a novel biomarker for p53 pathway activation. Mol. Cancer Ther. 2, 1023–1029.

Yasukawa, T., Suzuki, T., Ueda, T., Ohta, S., Watanabe, K., 2000. Modification defect at anticodon wobble nucleotide of mitochondrial tRNAs(Leu)(UUR) with pathogenic mutations of mitochondrial myopathy, encephalopathy, lactic acidosis, and stroke-like episodes. J. Biol. Chem. 275, 4251–4257.

Zhang, X.D., Qin, Z.H., Wang, J., 2010. The role of p53 in cell metabolism. Acta Pharmacol. Sin. 31, 1208–1212.

Anti-neutral glycolipid antibodies in encephalomyeloradiculoneuropathy

Sayuri Shima, MD
Naoki Kawamura, MD
Tomomasa Ishikawa, MD
Hiromi Masuda, PhD
Chihiro Iwahara, PhD
Yoshiki Niimi, MD
Akihiro Ueda, MD, PhD
Kazuhiza Iwabuchi, PhD
Tatsuro Mutoh, MD, PhD

Correspondence to Dr. Mutoh: tmutoh@fujita-hu.ac.jp

ABSTRACT

Objective: The aim of this study was to review 4 patients with encephalomyeloradiculoneuropathy (EMRN) and assess for autoantibodies against neutral glycolipids.

Methods: We studied the progression of clinical, radiologic, neurophysiologic, and CSF findings, as well as anti-neutral glycolipid antibodies in sera.

Results: All patients developed acute or subacute motor weakness and impaired consciousness. Their CSF showed pleocytosis and high immunoglobulin G concentrations. MRI revealed lesions in the brain and spinal cord. Neurophysiologic examinations indicated dysfunction of the spinal cord, nerve roots, and peripheral nerves. Steroid pulsed immunotherapy and/or high dose of IV immunoglobulin replacement therapy resulted in clear and often dramatic clinical improvements. Reactivity to anti-neutral glycolipid antibodies was positive in all patients with acute EMRN but not in the recovery phase. Forty-seven age-matched patients with other neurologic disorders and 28 age-matched healthy volunteers tested negative for reactivity to anti-neutral glycolipid antibodies.

Conclusion: The resolution of radiologic and neurologic abnormalities and altered autoantibody titers against neutral glycolipids after immunotherapy suggest that EMRN is caused by an immune-mediated mechanism. These autoantibodies may be useful biomarkers for EMRN.
Neurology® 2014;82:114–118

GLOSSARY

EMRN = encephalomyeloradiculoneuropathy; **GalCer** = galactosylceramide; **GSL** = glycosphingolipid; **LacCer** = lactosylceramide; **PNS** = peripheral nervous system.

Cellular or humoral immunologic dysfunction is one cause of demyelinating disorders of the CNS and peripheral nervous system (PNS). There is evidence that sera of patients with CNS diseases, such as multiple sclerosis[1] and acute disseminated encephalomyelitis,[2] or PNS diseases have in vivo and in vitro reactivity against various components of the CNS and PNS.[1]

The literature contains descriptions of patients with encephalomyeloradiculoneuropathy (EMRN).[3,4] Some authors have portrayed EMRN as acute disseminated encephalomyelitis with Guillain-Barré syndrome or as combined central and peripheral inflammatory demyelination.[5,6]

We previously reported antibodies against glucosylceramide in the sera of patients with relapsing polychondritis with limbic encephalitis.[7] Herein, we describe 4 patients with EMRN whose sera tested positive for anti-neutral glycosphingolipid (GSL) antibodies.

METHODS

Patient 1. A 50-year-old woman was hospitalized for viral meningitis after a flu-like illness, and 1 month later was transferred to our hospital because of worsening symptomatology. Examination revealed decreased level of consciousness, tetraplegia, and hyperreflexia without pathologic reflexes, left-sided Horner syndrome, facial hyperesthesia, and urinary incontinence (table). Serum autoantibodies, anti–aquaporin-4 antibody tests, antiviral antibody titers, and real-time PCR assays were negative. CSF findings were abnormal (table). Brain fluid-attenuated inversion recovery–weighted and T2-weighted MRI showed lesions with high signal intensity (figure 1A), and brain SPECT showed increased uptake in the same regions (figure 1C). Cervical MRI revealed an edematous spinal cord and long cord lesions with high signal intensity (figure 1B). Nerve conduction studies showed decreased amplitude of compound muscle action potentials and sensory nerve action potentials with absence of F waves in several nerves. Auditory brainstem response and somatosensory evoked potential were also abnormal.

Supplemental data at www.neurology.org

From the Department of Neurology (S.S., N.K., T.I., Y.N., A.U., T.M.), Fujita Health University School of Medicine, Aichi; and Institute for Environmental and Gender Specific Medicine (H.M., C.I., K.I.), Juntendo University Graduate School of Medicine, Chiba, Japan.
Go to Neurology.org for full disclosures. Funding information and disclosures deemed relevant by the authors, if any, are provided at the end of the article.

Table Clinical characteristics of 4 patients with EMRN

	Patient 1	Patient 2	Patient 3	Patient 4
Age, y/sex	50/F	49/M	26/M	76/F
Antecedent event	Viral meningitis	Flu	Flu	—
Weakness, MRC scale	2-3	3-4	2-3	4-5
GCS score on admission	11 (2-4-5)	11 (2-4-5)	11 (2-4-5)	14 (3-5-6)
Autonomic dysfunction	+ (inconti., Horner syndrome)	+ (ileus, inconti., unstable BP)	+ (inconti.)	+ (unstable BP, constipation)
Cell no. in CSF /mm^3	109	116	70	43
Protein level/IgG in CSF, mg/dL	81/10	192/43	173/19	65/12
Real-time PCR in CSF (EBV, HSV, CMV, HHV6, 7)	–	–	–	–
Neurophysiologic study	Mainly A	A + D	Mainly A	A + D
CMAP and SNAP↓	+	+	+	+
NCV↓	–	+	–	+
F-wave frequency, %	0	0	0	0
ABR, SEP abnormality	+	+	+	+
Antibody titer in sera LacCer/GalCer/GlcCer	2+/–/–[a]	3+/1+/–[a]	2+/±/–[a]	2+/–/–[a]

Abbreviations: A = axonal; ABR = auditory brainstem response; BP = blood pressure; CMAP = compound muscle action potential; CMV = cytomegalovirus; D = demyelination; EBV = Epstein-Barr virus; EMRN = encephalomyeloradiculoneuropathy; GalCer = anti-galactosylceramide antibody in serum; GCS = Glasgow Coma Scale; GlcCer = anti-glucosylceramide antibody in serum; HHV6 = human herpesvirus 6; HHV7 = human herpesvirus 7; HSV = herpes simplex virus; IgG = immunoglobulin G; inconti. = urinary incontinence; LacCer = lactosylceramide; MRC = Medical Research Council; NCV = nerve conduction velocity; SEP = somatosensory evoked potential; SNAP = sensory nerve action potential.
↓ = reduction.
[a] Optical density ratio: >3 3+; 2< 2+ <3; 1< 1+ <2; 0.3< ± <1; 0.3< –.

Figure 1 Serial neuroradiologic images for patient 1

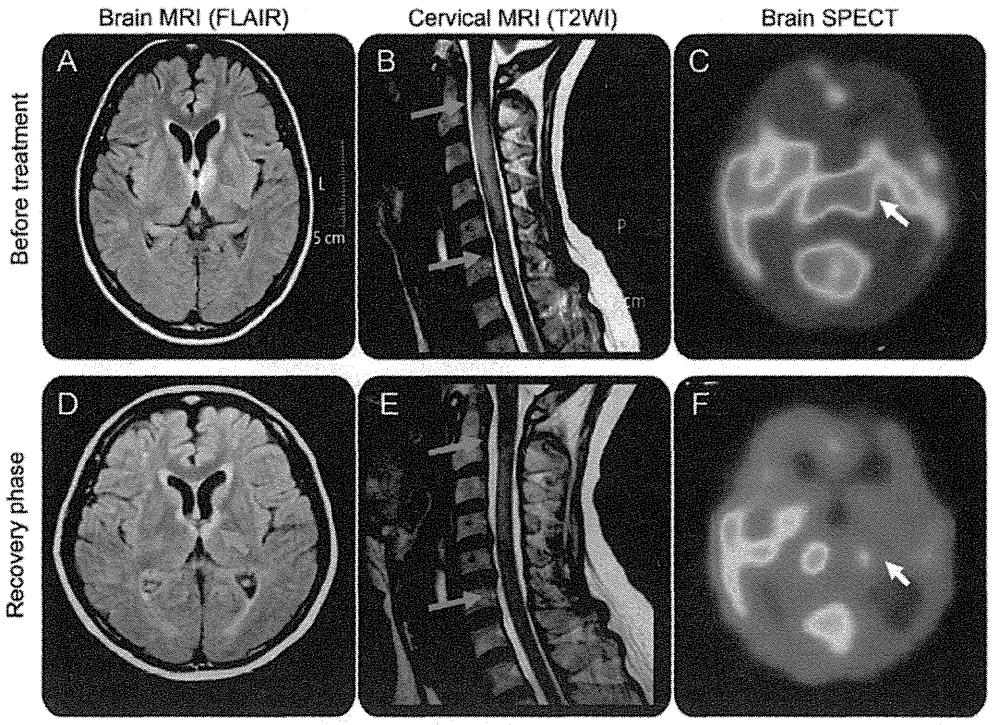

(A) Axial fluid-attenuated inversion recovery (FLAIR)-weighted brain MRI. (B) Sagittal T2-weighted (T2WI) cervical spinal cord MRI. (C) Brain SPECT obtained on day 3. (D–F) The same examinations obtained on day 52. The areas of high signal intensity on both the brain and spinal cord MRI on day 3 resolved by day 52. Arrows indicate lesions with high signal intensity on brain MRI that corresponded to high uptake areas on brain SPECT.

Figure 2 **Representative Far-Eastern blotting of neutral GSLs, and preabsorption of serum samples with a mixture of LacCer, GalCer, and GlcCer followed by Far-Eastern blot analysis**

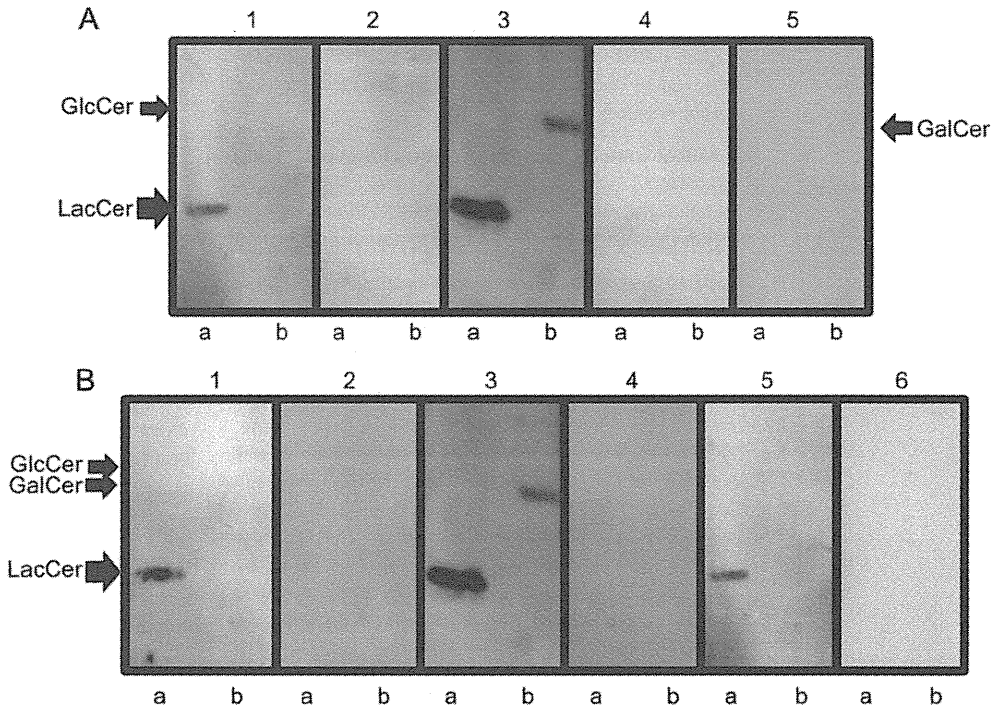

(A) Purified GlcCer, GalCer, and LacCer processed by thin-layer chromatography were electrothermally blotted onto a polyvinylidene difluoride membrane (Far-Eastern blotting). The membrane was probed with serum samples from patient 1 obtained before (1) and after (2) combined immunotherapy, serum samples from patient 2 before (3) and after (4) combined immunotherapy, and serum from a healthy volunteer (5). The position of each neutral glycolipid was determined on a thin-layer chromatography plate stained with anisaldehyde reagent.[9] We performed these experiments at least 3 times using different serum samples, with essentially identical results. Representative blots are shown. Note that serum obtained before immunotherapy from patient 1 was only positive for LacCer (immunoglobulin G fraction), whereas serum from patient 2 was positive for LacCer and to a lesser extent GalCer (immunoglobulin G fraction). In contrast, serum samples obtained from patients with EMRN after treatment and from 28 healthy volunteers showed no reactivity against these GSLs. Arrows indicate positions of LacCer, GlcCer, and GalCer. (B) Serum samples from patients with EMRN were preabsorbed with 0.1 μg each of the 3 neutral GSLs (LacCer, GalCer, and GlcCer) at 37°C for 30 minutes. These preabsorbed samples were used for further analysis. Serum from patient 4 before (1) and after (2) preabsorption with neutral GSLs, from patient 2 before (3) and after (4) preabsorption, and from patient 1 before (5) and after (6) preabsorption was used for further analysis. Serum preabsorbed with neutral GSLs was not reactive against these antigens, suggesting that antibodies against these glycolipids caused initial positive reactivity. These experiments were performed at least 3 times with essentially identical results. Representative results are shown. Arrows indicate positions of LacCer, GlcCer, and GalCer. EMRN = encephalomyeloradiculoneuropathy; GalCer = galactosylceramide; GlcCer = glucosylceramide; GSL = glycosphingolipid; LacCer = lactosylceramide.

We administered steroid pulse therapy (1,000 mg/d) for 3 days followed by high-dose IV immunoglobulin (0.4 g/kg/d) for 5 days. The patient's clinical condition and CSF, MRI, and SPECT findings improved (figure 1, D–F). She was fully recovered after 6 months.

Patient 2. A 49-year-old man was hospitalized because of a decreased level of consciousness, 1 week after the onset of flu-like symptoms. Neurologic examination revealed left facial nerve palsy, autonomic dysfunction, and tetraplegia with generalized hyperreflexia (table). Laboratory examination showed mild inflammatory reaction, but no autoantibodies. Brain gadolinium-enhanced T1-weighted images showed increased signal intensity along the meninges, and cervical MRI showed an edematous spinal cord. SPECT showed increased uptake in the right temporal and parietal lobes. Neurophysiologic and CSF examination findings were abnormal (table). After immunomodulatory treatment, the patient rapidly became alert and the radiologic abnormalities resolved.

Patient 3. The clinical findings of this 26-year-old man are shown in the table. His laboratory data were normal except for an abnormal antidiuretic hormone level. Brain MRI showed lesions with high signal intensity in the corpus callosum, and we noted increased cerebral blood flow on SPECT.

On the fourth hospital day, the patient became deeply comatose and required mechanical ventilation. After immunomodulatory treatment, his motor weakness improved and his respiratory dysfunction resolved. After 2 months, all neurophysiologic and radiologic abnormalities resolved.

Patient 4. The clinical details of this 76-year-old woman are shown in the table. The patient had abducens nerve palsy and autonomic dysfunction. Laboratory data were negative, but neurophysiologic examination findings were abnormal. We saw no lesions on brain MRI.

After IV immunoglobulin treatment, the patient's cranial nerve dysfunction resolved and her sensory and motor function gradually improved over the following month.

Sera from patients and healthy volunteers. Sera were obtained from freshly clotted blood and stored immediately in aliquots at −80°C until assayed. For comparison, we obtained serum samples from 47 age- and sex-matched patients with other neurologic disorders (8 with multisystem atrophy, 4 with neuromyelitis optica, 20 with chronic inflammatory demyelinating polyradiculoneuropathy, and 15 with multiple sclerosis) and from 28 age-matched healthy volunteers.

Standard protocol approvals, registrations, and patient consents. All study participants provided written informed consent for inclusion in this study. The Review Boards for Bioethics of Fujita Health University and Juntendo University approved this study.

Far-Eastern blot analyses using human sera. Far-Eastern blot analyses were performed using both acidic and neutral GSLs (Matreya, Pleasant Gap, PA) as described previously.[8,9] Polyvinylidene difluoride membrane was treated with human sera (×500 to ×2,000 dilution) in blocking buffer (2% nonfat milk in phosphate-buffered saline containing 1% Triton X-100). After treatment with a second antibody, positive bands were detected using enhanced chemiluminescence (PerkinElmer Inc., Boston, MA). To examine antigen identity, we incubated sera with a mixture of 0.1 μg each of neutral GSLs for 30 minutes at 37°C, and these preabsorbed sera were used for Far-Eastern blot analysis.[10] For quantification, we subjected all membranes to image analysis using NIH Image software, calculating the ratio of signal intensity to background intensity as previously described.[10]

Surface plasmon resonance analysis. See appendix e-1 on the *Neurology*® Web site at www.neurology.org.

RESULTS Clinical summary. The table shows the clinical details of the 4 patients with EMRN. All had acute or subacute motor weakness, acutely or subacutely decreased level of consciousness, brainstem dysfunction, and mild CSF pleocytosis, as well as negative antiviral antibody titers (including HIV) and real-time PCR assays for viral genomes in the CSF.

Detection of anti-neutral GSL antibodies. In all patients with EMRN, acute-phase serum samples showed clear positive bands corresponding to lactosylceramide (LacCer) (figure 2A, lane 1). In 2 patients, we noted a weak band corresponding to galactosylceramide (GalCer) (figure 2A, lane 3). In contrast, recovery-phase serum samples did not show reactivity against neutral GSLs (figure 2A, lanes 2 and 4). Patients with other neurologic disorders and 28 healthy volunteers did not have reactivity against neutral GSLs (data not shown). Anti-neutral GSL antibody titers are shown in the table.

Serum samples that were preabsorbed with a mixture of neutral GSLs did not show any positive bands, suggesting that initial positive reactivity was caused by antibodies against these GSLs (figure 2B, lanes 2, 4, and 6). Acute-phase CSF of patients with EMRN was weakly positive for GalCer and none of the sera had positive reactivity against any gangliosides (data not shown).

Surface plasmon resonance analysis. Surface plasmon resonance examination of serum samples from patients with EMRN showed antibodies against LacCer (figure e-1, patient 1) and to a lesser extent GalCer (figure e-1, patients 2 and 3). Control serum samples did not show any reactivity (figure e-1).

DISCUSSION The predominant symptoms we observed in the 4 patients with EMRN were acute motor weakness and a decreased level of consciousness. Radiologic examinations showed abnormalities of the brain and spinal cord, and electrophysiologic studies indicated dysfunction of the spinal cord, nerve roots, and peripheral nerves. Very few cases of EMRN have been reported, and most responded well to immunotherapy, similar to the patients described herein.[3,4]

GalCer is a major GSL in the cell membranes of myelin-forming cells such as oligodendrocytes and Schwann cells. Anti-GalCer antibody causes a demyelinating disorder of the PNS in rabbits.[e1] LacCer is distributed throughout the body, including the CNS, PNS, and peripheral blood cells such as neutrophils.[e2–e5] In human neutrophils, binding of anti-LacCer antibody to the LacCer domains stimulates superoxide production and phagocytosis.[e5] Although this report involves a small number of patients, our results strongly suggest that anti-neutral GSL antibodies can be used as biomarkers for EMRN.

AUTHOR CONTRIBUTIONS

Dr. Shima performed data acquisition, analysis, and manuscript drafting. Drs. Kawamura, Ishikawa, Niimi, and Ueda performed patient evaluation, data acquisition, and analysis. Drs. Masuda, Iwahara, and Iwabuchi analyzed and interpreted surface plasmon resonance analysis data. Dr. Mutoh was involved in study design, scientific supervision, and drafting and revising of the manuscript.

STUDY FUNDING

Partly supported by a grant-in-aid for the MEXT-Supported Program for the Strategic Research Foundation at Private Universities and Scientific Research (C) from the Ministry of Education, Culture, Sports, Science and Technology of Japan, and a Research Grant for Intractable Diseases from the Ministry of Health, Labor and Welfare of Japan to T.M.

DISCLOSURE

The authors report no disclosures relevant to the manuscript. Go to Neurology.org for full disclosures.

Received May 15, 2013. Accepted in final form September 26, 2013.

REFERENCES

1. Lisak RP, Zweiman B, Burns JB, et al. Immune responses to myelin antigens in multiple sclerosis. Ann NY Acad Sci 1984;436:221–230.
2. Kesselring J, Miller DH, Robb SA, et al. Acute disseminated encephalomyelitis: MRI findings and the distinction from multiple sclerosis. Brain 1990;113:291–302.
3. Blennow G, Gamstrop I, Rosenberg R. Encephalo-myeloradiculo-neuropathy. Dev Med Child Neurol 1968;10:485–490.
4. Itokazu N, Kodama Y, Kontani S, et al. A case of acute polyradiculoneuritis with multiple cranial nerve palsy and cerebral lesion: possible evidence of encephalo-myeloradiculo-neuropathy. Brain Dev 1998;30:423–429.

5. Kinoshita K, Hayashi M, Miyamoto K, Oda M, Tanabe H. Inflammatory demyelinating polyradiculitis in a patient with acute disseminated encephalomyelitis (ADEM). J Neurol Neurosurg Psychiatry 1996;60:87–90.
6. Rubin M, Karpati G, Carpenter S. Combined central and peripheral myelinopathy. Neurology 1987;37:1287–1290.
7. Mihara T, Mutoh T, Yoshikawa T, et al. Postinfectious myeloradiculoneuropathy with cranial nerve involvements associated with human herpesvirus 7 infection. Arch Neurol 2005;62:1755–1757.
8. Mihara T, Ueda A, Hirayama M, et al. Detection of new anti-neutral glycosphingolipids antibodies and their effects on Trk neurotrophin receptors. FEBS Lett 2006;580:4991–4995.
9. Mutoh T, Kawamura N, Hirabayashi Y, et al. Abnormal cross-talk between mutant presenilin 1 (I143T, G384A) and glycosphingolipid biosynthesis. FASEB J 2012;26:3065–3074.
10. Ueda A, Shima S, Miyashita T, et al. Anti-GM1 antibodies affect the integrity of lipid rafts. Mol Cell Neurosci 2010;45:355–362.